THE JOURNAL OF BIOLOGICAL CHEMISTRY VOL. 288, NO. 36, pp. 25880–25894, September 6, 2013

Subunit δ Is the Key Player for Assembly of the H^+-translocating Unit of *Escherichia coli* F_OF_1 ATP Synthase*

Received for publication, May 10, 2013, and in revised form, July 16, 2013 Published, JBC Papers in Press, July 17, 2013, DOI 10.1074/jbc.M113.484675

Florian Hilbers[1,2], **Ruth Eggers**[1,3], **Kamila Pradela, Kathleen Friedrich, Brigitte Herkenhoff-Hesselmann, Elisabeth Becker**[4], **and Gabriele Deckers-Hebestreit**[5]

From the Department of Microbiology, University of Osnabrück, Barbarastrasse 11, D-49069 Osnabrück, Germany

Background: F_OF_1 ATP synthases are rotary nanomachines transporting protons across the membrane during catalysis.
Results: *Escherichia coli* F_OF_1 is assembled from subcomplexes with subunit δ functioning as clamp to generate stable F_O.
Conclusion: δ guarantees that the open proton channel is concomitantly assembled within coupled F_OF_1.
Significance: We investigate how a proton-translocating unit is assembled while simultaneously maintaining the low membrane proton permeability essential for viability.

The ATP synthase (F_OF_1) of *Escherichia coli* couples the translocation of protons across the cytoplasmic membrane to the synthesis or hydrolysis of ATP. This nanomotor is composed of the rotor $c_{10}\gamma\epsilon$ and the stator $ab_2\alpha_3\beta_3\delta$. To study the assembly of this multimeric enzyme complex consisting of membrane-integral as well as peripheral hydrophilic subunits, we combined nearest neighbor analyses by intermolecular disulfide bond formation or purification of partially assembled F_OF_1 complexes by affinity chromatography with the use of mutants synthesizing different sets of F_OF_1 subunits. Together with a time-delayed *in vivo* assembly system, the results demonstrate that F_OF_1 is assembled in a modular way via subcomplexes, thereby preventing the formation of a functional H^+-translocating unit as intermediate product. Surprisingly, during the biogenesis of F_OF_1, F_1 subunit δ is the key player in generating stable F_O. Subunit δ serves as clamp between ab_2 and $c_{10}\alpha_3\beta_3\gamma\epsilon$ and guarantees that the open H^+ channel is concomitantly assembled within coupled F_OF_1 to maintain the low membrane proton permeability essential for viability, a general prerequisite for the assembly of multimeric H^+-translocating enzymes.

F_OF_1 ATP synthases comprise different structural and functional entities that couple the translocation of ions across the membrane to the synthesis or hydrolysis of ATP via a rotary mechanism. In *Escherichia coli*, the membrane-integrated, H^+-translocating F_O complex consists of subunits ab_2c_{10}, whereas the peripherally associated F_1 part with its catalytic centers comprises subunits $\alpha_3\beta_3\gamma\delta\epsilon$. As the rotor $c_{10}\gamma\epsilon$ is driven by the transport of protons through two half-channels formed by subunit *a* as well as the c_{10} ring in F_O, the rotation of $\gamma\epsilon$ causes conformational changes in the catalytic nucleotide-binding sites within the $\alpha_3\beta_3$ hexamer of F_1, thereby provoking ATP synthesis and its release. To counter the tendency of the $\alpha_3\beta_3$ to follow the rotation of the rotor, a peripheral stalk consisting of $b_2\delta$ stabilized by subunit *a* acts as a stator and holds $\alpha_3\beta_3$ in position (1, 2).

In *E. coli*, insertion of subunit *c* into the membrane depends on YidC insertase (3), and formation of a c_{10} subcomplex is independent of the presence of other F_OF_1 subunits (4). Recent studies on AtpI revealed a participation probably in a chaperone-like manner in the assembly of a stable *c* ring (5–7). Insertion of subunits *a* and *b* into the membrane involves the Sec translocon, the signal recognition particle pathway, and for subunit *a* also YidC (8–10). Furthermore, a stable insertion of subunit *a* into the membrane is strictly dependent upon the co-insertion of the other F_O subunits, whereas *b* and *c* are inserted independently (11). Overexpression of subunits α, β, and γ allowed complex formation with high ATPase activity in the cytoplasm (12), and for interaction between subunits δ and α, the assembly of α with other F_1 subunits is a prerequisite (13).

The different subunits of *E. coli* ATP synthase are translated from a polycistronic *atp* mRNA, and a balanced stoichiometry is obtained by translational coupling between the cistrons as well as regulation by mRNA secondary structure (14, 15). In most bacteria, the cistrons are arranged in clusters separating those for F_O from those for F_1, an arrangement fitting well with the proposal that both have been evolved from functionally unrelated ancestor protein complexes (16–18). Furthermore, this suggests that ATP synthases are probably assembled from subcomplexes, and studies on the assembly of the yeast mitochondrial ATP synthase support this assumption (19).

The goal of this study was to gain insight into the assembly pathway of the F_O complex of the *E. coli* ATP synthase with special emphasis on the H^+-translocating unit. Accordingly, the analyses of single-subunit knock-out mutants Δ*a*, Δ*b*, and Δδ, in which the synthesis of subunits *a*, *b*, and δ, respectively, is prevented due to insertion of an early stop codon into the corresponding gene, were combined with intermolecular disulfide bond formation of cysteine-substituted subunits or affinity purification of partially assembled F_OF_1 complexes. Δ*a* allowed

* This work was supported by Deutsche Forschungsgemeinschaft Grant DE482/1-1.
[1] Both authors contributed equally to this work.
[2] Present address: Dept. of Molecular Biology and Genetics, Aarhus University, Gustav Wieds Vej 10c, DK-8000 Aarhus, Denmark.
[3] Present address: Korea Institute of Science and Technology, Forschungsgesellschaft mbH, Campus E7.1, D-66123 Saarbrücken, Germany.
[4] Present address: Heinrich-Heine-Universität Düsseldorf, Funktionelle Genomforschung der Mikroorganismen, Universitätsstrasse 1, D-40225 Düsseldorf, Germany.
[5] To whom correspondence should be addressed. Tel.: 49-541-969-2809; Fax: 49-541-969-3942; E-mail: deckers-hebestreit@biologie.uni-osnabrueck.de.

the formation of F_OF_1-a in amounts comparable with wild type. Δδ revealed the presence of an ab_2 as well as a $c_{10}\alpha_3\beta_3\gamma\epsilon$ subcomplex; both could be assembled into a functional ATP synthase by a time-delayed synthesis of subunit δ. Δ*b* only contained the F_OF_1 core complex $c_{10}\alpha_3\beta_3\gamma\epsilon$. In each case, subunit δ was essential for the integration of the *b* dimer into the core complex independent of the interaction of b_2 with subunit *a*. This demonstrates that δ functions as a clamp between ab_2 and $c_{10}\alpha_3\beta_3\gamma\epsilon$ to generate the H^+-translocating machinery within F_O.

EXPERIMENTAL PROCEDURES

Mutagenesis—All plasmids used are listed in Table 1. In most cases, a two-step PCR method was used to generate the early stop codons and the cysteine substitutions in the individual subunits. For cysteine substitutions, the plasmids used as template DNA contain alanine codons instead of the endogenous cysteine codons in the *atp* genes mutated. Mutant PCR fragments were transferred into pBWU13 or its derivatives using single or double cutters for restriction. To study subunit interactions in the absence of other F_OF_1 subunits, *atpF* or *atpEF* were cloned into plasmid pET-22b via NdeI/EcoRI with the EcoRI site directly located downstream of the corresponding stop codon. For expression of the *atp* genes under control of the inducible/repressible promoter P_{araBAD}, a KpnI site was introduced in pFV2 downstream of the weak, constitutive *atp* promoter P3 (29). Subsequently, the *atp* operon was cloned into pBAD33 via KpnI (49 bp upstream of the stop codon of *atpI*) and XbaI (320 bp downstream of the 3′-end of *atpC*). The *atpH* gene was cloned into plasmid pET-22b via NdeI/EcoRI, and the start codon was subsequently exchanged to TTG. The presence of each mutation was confirmed by DNA sequencing.

Bacterial Strains and Growth Conditions—E. coli strains used are listed in Table 1. The *atp* deletion strain HB1(DE3) was obtained by P1 co-transduction of Δ*atpBEFHAGDC* and *ilv*::*Tn*10 (Tet^R) using DK8 (20) as donor and BL21(DE3) (Novagen) as recipient strain (4). *E. coli* strain DK8 transformed with plasmid pBWU13 or its derivatives or strain HB1(DE3) transformed with pET-22b derivatives were grown in minimal medium with 0.5% (v/v) glycerol or in LB medium with 100 μg/ml ampicillin as described (4). All DK8 cells transformed with pBWU13 derivatives grew on succinate as a nonfermentable carbon source indicating a functional oxidative phosphorylation system, whereas no growth was observed in knock-out mutants (data not shown).

Time-delayed in Vivo Assembly of Subunit δ into Preformed $F_OF_1-\delta$—The time-delayed *in vivo* assembly system used to study the time-delayed integration of subunit δ into preformed F_OF_1 subcomplexes missing subunit δ has been characterized in detail by Brockmann *et al.* (30). DK8 transformed with three different plasmids was grown in TYGPN medium (31) at 37 °C with 100 μg/ml ampicillin, 30 μg/ml chloramphenicol, and 50 μg/ml kanamycin. The medium was preincubated overnight with 10 units/ml β-galactosidase from *Kluyveromyces lactis* (Sigma) for removal of lactose known to be present in varying amounts in yeast extract used for preparation of TYGPN medium (TaKaRa Single Protein Production System, TaKaRa Bio Inc.). After inoculation, the medium was supplemented with 0.03% (w/v) arabinose for induction of P_{araBAD}-controlled *atp* genes. At $OD_{578\,nm}$ = 0.3, the *araBAD* promoter was repressed by adding 0.5% (w/v) glucose and 0.045% (w/v) D-fucose (33, 24). After degradation of *atp* mRNA within 20 min, the expression of *atpH* and T7 *gene1* (28) was induced by the addition of 0.1 mM IPTG[6] for 1 h.

RNA Extraction, cDNA Synthesis, and rt-RT-PCR—2.5×10^8 cells (as calculated according to the finding of Neidhardt *et al.* (34) that 1 ml of cells contains 10^9 viable cells at OD = 1.0) were mixed with 2 volumes of RNAprotect bacteria reagent (Qiagen), incubated for 5 min at room temperature, harvested at 5,000 × *g*, and stored at −20 °C. RNA extraction, synthesis of cDNA, and rt-RT-PCR were performed as described (30, 35) using the following primer pairs: *atpE′F* (5′-CAGGCGCAGGCGGAAATTG-3′ (bp 1626–1645) and 5′-CCGTAATAAATTCAGACATCAGCCCC-3′ (bp 1821–1796)) and *atpA* (5′-GCGAACTGATCAAGCAGCGC-3′ (bp 2374–2393) and 5′-ACCCATAACAACCGCACCTAC-3′ (bp 2579–2559)). The primer annealing sites are indicated in parentheses according to the numbering of plasmid pBWU13 (21), starting with 1 at the second HindIII restriction site in *atpI*. The calculated threshold cycle values were normalized against those of housekeeping gene *rpsL* (5′-GGTACGCAAACCACGTGCTCG-3′ and 5′-CAGGTTGTGACCTTCACCACC-3′) (30).

Copper Cross-linking—Inverted membrane vesicles were prepared in the presence of protease inhibitor mix without EDTA (Sigma) according to Krebstakies *et al.* (23) using TMG buffer (50 mM Tris-HCl, pH 7.5, 10 mM $MgSO_4$, 10% (v/v) glycerol). Cross-linking of membrane vesicles was carried out as described by Ballhausen *et al.* (4), incubating 5 mg/ml membrane protein in the presence of 1.5 mM copper-1,10-phenanthroline (CuP) in TMG, pH 7.5 or pH 8.2, for 1 h at 23 °C. The reaction was stopped by the addition of 50 mM EDTA and 25 mM *N*-ethylmaleimide, and after 20 min, a quarter volume of 4× SDS sample buffer without 2-mercaptoethanol (36) was added.

Purification of Polyhistidine-tagged Proteins—For isolation of F_OF_1 via a His_6 tag fused N-terminally to subunit β, membranes were prepared from a 3-liter cell culture according to Wise *et al.* (37), and membrane proteins were extracted as described by Pänke *et al.* (38). After centrifugation, the solubilized proteins were incubated for 1.5 h on ice with 1 ml of Ni^{2+}-nitrilotriacetic acid-Sepharose FF (GE Healthcare). Subsequently, the matrix was washed with 50 mM Tris-HCl, pH 7.5, 5 mM $MgCl_2$, 1% (w/v) *n*-octyl-β-D-glucopyranoside, 20 mM imidazole, 10% (v/v) glycerol and eluted with the same buffer containing 150 mM imidazole.

The solubilization of F_OF_1 with a His_{12} tag fused N-terminally to subunit *a* was performed according to Krebstakies *et al.* (22). 5 mg of membranes prepared in TMG buffer were pelleted, resuspended in 50 mM Tris-HCl, pH 7.5, 10% (v/v) glycerol, 0.1 mM PMSF, 1.4% (w/v) *n*-dodecyl-β-D-maltoside, and

[6] The abbreviations used are: IPTG, isopropyl-β-D-thiogalactopyranoside; ACMA, 9-amino-6-chloro-2-methoxyacridine; Ara, L-arabinose; CuP, copper-1,10-phenanthroline; DCCD, *N*,*N*′-dicyclohexylcarbodiimide; Fuc, D-fucose; OD, optical density measured at 578 nm; OSCP, oligomycin sensitivity-conferring protein; rt-RT-PCR, real-time RT-PCR; TMG, Tris/magnesium/glycerol.

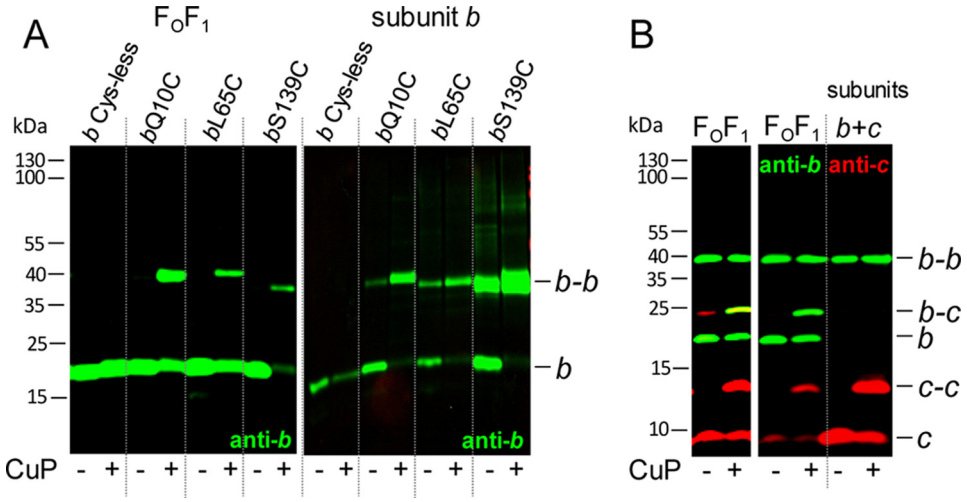

FIGURE 1. **Comparison of cross-linked subunit *b* or subunits *b* and *c* in membranes of cells expressing the *atp* operon (F_OF_1) and cells exclusively expressing *atpF* (subunit *b*) or *atpEF* (subunits *b* and *c*).** *A*, cross-linking of subunit *b*. F_OF_1, DK8 transformed with pBWU13 derivatives (*b* Cys-less, pSTK3; *b*Q10C, pBH16; *b*L65C, pSTK8; *b*S139C, pBH17) were grown in minimal medium with 0.5% (v/v) glycerol and harvested at OD = 0.8–1.0. *subunit b*, cells of *E. coli* HB1(DE3) transformed with pET-22b derivatives (*b*Q10C, pET22-atpF1; *b*L65C, pET22-atpF3; *b*S139C, pET22-atpF2) were grown in LB medium with ampicillin to OD = 0.6 prior to induction of *atpF* gene expression with 1 mM IPTG for 1 h. Membranes (20 μg of protein/lane) containing cysteine-substituted subunit *b* were separated after cross-linking with CuP at pH 8.2 by non-reducing SDS-PAGE and analyzed by immunoblotting. *B*, cross-linking of subunits *b* and *c*. F_OF_1, DK8 transformed with pHB3 (*b*N2C/*c*V74C); *subunits b* + *c*, cells of HB1(DE3) transformed with pET22-atpEF1 (*b*N2C/*c*V74C) were grown and analyzed as described in *A*. Using the Odyssey system, the intensities of the fluorescence detected in the individually immunolabeled bands are adjusted between a minimum and a maximum for each blot membrane scanned and separately for both detection channels. Due to the extremely high intensity of the *red*-labeled *c* and *c*-*c* bands of the membranes containing only subunits *b* and *c* (*right*), it was not possible to verify the presence of subunits *b* and *c* in the *b*-*c* cross-link band of F_OF_1-containing membranes. Therefore, the *left panel* shows F_OF_1 of the same immunoblot after cropping the *right part* of the *right panel* to readjust the intensities of the fluorescence.

stirred for 30 min at 16 °C. After centrifugation, the supernatant was adjusted to 150 mM NaCl, 0.1 mM PMSF, and 20 mM imidazole (pH 7.5) and incubated end-over-end for 15 min with the matrix of a His SpinTrap™ column (GE Healthcare). Handling was performed as recommended by the supplier using 50 mM Tris-HCl, pH 7.5, 10% (v/v) glycerol, 0.1 mM PMSF, 150 mM NaCl, 20 mM imidazole, 1% (w/v) sodium cholate as binding buffer and the same buffer containing 500 mM imidazole as elution buffer. All buffers used included protease inhibitor mix without EDTA.

Assays—Protein concentrations were determined with the BCA assay (Pierce). Proteins were separated by SDS-PAGE using 10% separating gels (39) with PageRuler™ prestained protein ladder (Fermentas) as standard. Immunoblotting was performed according to Birkenhäger *et al.* (40). For immunolabeling, polyclonal antibodies raised in mice (anti-α, anti-β, anti-δ, anti-ϵ) or rabbits (anti-α, anti-β, anti-γ, anti-*b*, anti-*c*) and monoclonal antibodies raised in rat (anti-γ) or mice (anti-*a*, anti-*b*, anti-*c*) against the individual subunits of F_OF_1 were used as primary antibodies as indicated in the figures. IRDye™800DX-labeled goat-anti-mouse IgG, IRDye™800DX-labeled goat-anti-rat IgG, or IRDye™700DX-labeled goat-anti-rabbit IgG (Rockland) was applied as secondary antibody and detected with the two-channel system Odyssey (LI-COR). The secondary antibodies are affinity-purified for low cross-reactivities, and they allowed the simultaneous detection of fluorescence (shown in red or green) after immunolabeling of two proteins on one blot membrane. In the case of cross-linking of two different proteins, an overlay of both labels appears as a yellow band. Due to the varying avidities of the antibodies used, the color of the yellow bands may change to orange or lime green.

ATPase activities of membrane vesicles were determined as described (41). ATP- and NADH-driven proton pumping via ACMA fluorescence quenching was performed according to Birkenhäger *et al.* (40).

RESULTS

Formation of b Dimer Independent of Other F_OF_1 Subunits—To investigate the formation of the *b* dimer in the absence of other F_OF_1 subunits, we performed nearest neighbor analyses by use of disulfide bond formation after substituting a single amino acid residue within the polypeptide chain to cysteine. We have chosen three cysteine substitutions that are spread over the polypeptide chain, namely *b*Q10C, *b*L65C, and *b*S139C, and compared the *b*-*b* formation in the presence and absence of other F_OF_1 subunits. CuP was applied for generation of disulfide bonds using membranes with a *b*C21A substitution as a Cys-less control. Cross-linking was analyzed by immunoblotting after non-reducing SDS-PAGE (Fig. 1*A*). The cross-linking yields obtained for *b*-*b* assembled in F_OF_1 (Fig. 1*A*, *left*) were comparable with those described previously (42–44). For *b*S139C, a nearly complete removal of monomeric *b* was observed, indicating a high cross-linking yield; however, the signal of *b*-*b* was very low, and the apparent molecular mass was lower than that observed for the other *b*-*b* cross-linking products, as has also been observed by McLachlin and Dunn (44). Both results imply a different protein folding within *b*-*b* for *b*S139C compared with dimerization by residues *b*Q10C or *b*L65C.

In the absence of other F_OF_1 subunits, the immunoblot analysis also showed *b*-*b* formation with high cross-linking yields (Fig. 1*A*, *right*). In the presence of CuP, monomeric *b* was completely missing, and the cross-linking products were detected in comparable rates using the same antibody as described above.

However, for *b*S139C, the cross-linking product was split into two bands, indicating the presence of two different conformations for *b-b*, both comparable with the different apparent molecular masses found for cross-linking of subunit *b* in F_OF_1. Furthermore, for *b*L65C and *b*S139C, dimer formation could already be observed even without CuP as oxidant, suggesting that the interacting SH-groups are even susceptible to oxidation by oxygen. In conclusion, membrane-bound *b* subunits showed dimer formation independent of the presence of other F_OF_1 subunits.

No Interaction between b Dimer and the c_{10} Ring in the Absence of Other F_OF_1 Subunits—In the absence of other F_OF_1 subunits, individually synthesized, membrane-bound subunits *b* and *c* have been shown to be organized in homooligomeric subcomplexes; namely, the *c* subunits are arranged in a ring of 10 monomers (4), whereas the *b* subunits are present in dimeric form (Fig. 1*A*). To answer the question of whether both subcomplexes interact with each other, as observed in F_OF_1 using the *c*V74C/*b*N2C variant (25), the same experimental design as described above was used. For expression of individual subunits *b*N2C and *c*V74C, the modified genes *atpEF* were cloned in the same gene order, retaining the intergenic region as in the *atp* operon, and protein interaction was examined in membranes by oxidation with CuP. Despite massive overproduction of subunits *b* and *c* in the membranes due to the expression of these subunits with the pET system, no *b-c* cross-linking product could be detected in the corresponding immunoblot analysis (Fig. 1*B*), whereas *b-c* cross-linking was present in F_OF_1-containing membranes, as expected. In addition, *c-c* as well as *b-b* were monitored as a cross-linking side reaction. Although the proportion of monomeric and dimeric *c* subunits was comparable in both samples, although the expression level of subunit *c* is completely different, the dimerization of subunit *b* even in the absence of CuP as oxidant was unusually high (Fig. 1*B*), indicating that the flexible N-terminal region forced *b-b* formation when subunit *c* was not in close vicinity. In summary, the data demonstrate that the individually assembled membrane-bound subunit *b* dimer has no contact with the oligomeric c_{10} ring when both subunits are expressed simultaneously in the absence of other F_OF_1 subunits.

Presence of F_OF_1 Subunits in Membranes of Single-subunit Knock-out Mutants Δ*a,* Δ*b, and* Δδ—Subunit *a* and subunit δ are both known to be tightly bound to the subunit *b* dimer to stabilize the stator part of F_OF_1 *versus* the strong forces present during rotation of $c_{10}\gamma\epsilon$ in catalysis. Quantitative binding experiments revealed K_d values in the range of 2–3 nM for the $b\delta$ interaction in F_OF_1 (22), and an ab_2 subcomplex can be purified from wild type membranes via an N-terminal His_{12} tag fused to subunit *a* (41). To elucidate the need of subunit *a* and/or δ for the assembly of the *b* dimer into the F_OF_1 complex, we have constructed single-subunit knock-out mutants, in which one of the F_OF_1 subunits, namely *a*, *b*, or δ, is no longer synthesized. For that purpose, the Δ*atpB-C* strain DK8 was transformed with pBWU13 derivatives (Table 1) in which the synthesis of one of the eight F_OF_1 subunits was prevented due to insertion of an early stop codon into the corresponding gene of the otherwise unchanged *atp* operon. In mutant Δδ, the stop codon was inserted at codon 11 of the *atpH* gene (δY11end) and in Δ*b* at codon 7 of *atpF* (*b*I7end), whereas in Δ*a* the stop codon was introduced at codon position *a*W231, a mutation that has been well characterized (11, 45). Characterization of membranes of mutants Δ*a* and Δδ by immunoblotting revealed the presence of all F_OF_1 subunits except the one knocked out (Fig. 2*A*), indicating that the insertion of the additional stop codon induced no polar effect on the expression of the cistrons located downstream to the mutation in the polycistronic *atp* mRNA. However, it is important to note that no truncated subunit *a*W231end could be observed in all experiments performed, as has been discussed in detail by Hermolin and Fillingame (11).

In contrast, in membranes of Δ*b*, also subunits *a* and δ, which are tightly bound to the *b* dimer in F_OF_1, are completely missing in addition to subunit *b*. Such an interdependence between F_OF_1 subunits during assembly has been previously described for subunit *a* to be interdependent on subunits *b* and *c* (11, 46).

The immunoblot analysis (Fig. 2*A*) showed that in membranes of mutant Δ*a*, the amount of F_OF_1 subunits present was comparable with wild type, whereas it was largely reduced in membranes of Δ*b* and Δδ. To obtain roughly comparable signals in immunoblotting, we therefore increased the amount of protein for Δδ by a factor of 7. This fits very well for all F_OF_1 subunits except subunit *c*, which now revealed largely increased amounts of protein compared with wild type. For subunit *c*, comparable intensities for wild type and Δδ were obtained by separation of identical amounts of membrane protein, as can be observed for the Δ*b* mutant as well. Furthermore, intermolecular cross-linking via oxidation of bicysteine-substituted subunit *c* (*c*A21C/*c*M65C) (4, 47) produced an equal pattern of cross-link formation with all intermediate oligomers possible, stopping with the formation of decamers in either case (Fig. 2*B*). These observations demonstrate that the ringlike structure of the subunit *c* oligomer is not only independently assembled in the membrane (compare Refs. 4 and 47) but maintains high stability against degradation by proteases and is, therefore, present in Δδ and Δ*b* in amounts comparable with wild type in contrast to the other subunits of F_OF_1, indicating the presence of free c_{10} subcomplexes.

The ATPase activities of membrane vesicles of the knock-out mutants compared with wild type exhibited a similar behavior (Table 2). Although subunit *a* is missing and the proton pathway cannot be established (30), the ATPase activity of Δ*a* is in a range comparable with wild type activities, providing evidence for a stable assembly of the remaining F_OF_1 subunits. In membranes of Δδ and Δ*b*, the ATPase activities were reduced by a factor of 5–7, corresponding well to the amount of F_OF_1 proteins present in the membrane. In addition, the interaction areas of the $\alpha_3\beta_3$ hexamer with subunit γ were verified by disulfide bond formation. Membranes containing subunit pairs with single cysteine substitutions were applied, confirming contact sites between subunits α-γ (αA334C/γL262C) and β-γ (βD380C/γC87) (Fig. 2*B*) comparable with wild type (27). Therefore, it can be concluded that at least an F_OF_1 core complex composed of subunits $c_{10}\alpha_3\beta_3\gamma$ exhibiting ATPase activity is assembled in membranes of Δδ and Δ*b*.

Cross-linking of Subunit b with Its Interacting Subunits α, β, and c in Mutants Δ*a and* Δδ—In wild type F_OF_1, subunit *b* has contact with subunits *a* and *c* of F_O and subunits α, β, and δ of

TABLE 1
***E. coli* strains and plasmids**

E. coli strains and plasmids	Genotype/Description	Source/Reference
Strains		
DK8	*Hfr*PO1, *bglR, thi1, relA1, ilv*::*Tn*10 (Tet^R), Δ*atpBEFHAGDC*	Ref. 20
HB1(DE3)	F^-, *dcm, ompT, hsdS* (r_b^- m_b^-), *gal*, λ(DE3), *ilv*::*Tn*10 (Tet^R), Δ*atpBEFHAGDC*	Ref. 4
Plasmids		
pBWU13 derivatives		
pBWU13	Ap^R, pMB1 origin, *atpI′BEFHAGDC*	Ref. 21
pBH1	His_{12} tag N-terminally to *a*	Ref. 22
pBH7	His_6 (MRGSHHHHHHG) tag N-terminally to β	This study
pBH16	*b*Q10C, *b*C21A	This study
pBH17	*b*S139C, *b*C21A	This study
pBH20.1	*b*E155C, *b*C21A	This study
pBH26.1	αA334C, γL262C, αC47A, αC90A, αC193A, αC243A, γC87A, γC112A	This study
pBH29	βD380C, βC137A, γC112A	This study
pBH55.bα	*a*W231end, *b*A92C, αR477C, *b*C21A, αC47A, αC90A, αC193A, αC243A	This study
pBH55.bβ	*a*W231end, *b*A92C, βQ351C, *b*C21A, βC137A	This study
pBH55.β-His	*a*W231end, His_6 tag N-terminally to β	This study
pBH56.a-His12	δY11end, His_{12} tag N-terminally to *a*	This study
pBH56.bβ	δY11end, *b*A92C, βQ351C, *b*C21A, βC137A	This study
pBH56.β-His	δY11end, His_6 tag N-terminally to β	This study
pBH152	*a*N238C, *b*A13C, *b*E155C, *b*C21A	This study
pBH152.Δδ	δY11end, *a*N238C, *b*A13C, *b*E155C, *b*C21A	This study
pBWU13.Δb	*b*I7end	This study
pBWU13.Δδ	δY11end	This study
pBWU13.NOC	*c*A21C, *c*M65C, *b*C21A	Ref. 23
pHB3	*b*N2C, *c*V74C, *b*C21A	This study
pHB5	*a*W231end	This study
pHB15	*a*W231end, *b*N2C, *c*V74C, *b*C21A	This study
pHB17	*a*W231end, *b*L65C, *b*C21A	This study
pJGA3	*b*I7end, αP280C, γA285C, αC47A, αC90A, αC193A, αC243A, γC87A, γC112A	This study
pJGA4	*b*I7end, βD380C, βC137A, γC112A	This study
pJGA5.1	*b*I7end, *c*A21C, *c*M65C	This study
pJPKB.βQ351C	*b*A92C, βQ351C, *b*C21A, βC137A	Ref. 48
pKB1.αR477C	*b*A92C, αR477C, *b*C21A, αC47A, αC90A, αC193A, αC243A	Ref. 48
pKB7.aN238C	*a*N238C, *b*A13C, *b*C21A	This study
pRE2	δY11end, *b*N2C, *c*V74C, *b*C21A	This study
pRE3	δY11end, *c*A21C, *c*M65C, *b*C21A	This study
pRE4	δY11end, *b*L65C, *b*C21A	This study
pRE8	δY11end, αP280C, γA285C, αC47A, αC90A, αC193A, αC243A, γC87A, γC112A	This study
pRE10	δY11end, βD380C, βC137A, γC112A	This study
pRE14	δY11end, *b*A92C, αR477C, *b*C21A, αC47A, αC90A, αC193A, αC243A	This study
pSP2.a238/b13	δY11end, *a*N238C, *b*A13C, *b*C21A	This study
pSTK3	*b*C21A	This study
pSTK8	*b*L65C, *b*C21A	This study
pET-22b derivatives		
pET-22b	Ap^R, *lacI*, pMB1 origin	Novagen
pET-atpF1	*atpF*, *b*Q10C, *b*C21A	This study
pET-atpF2	*atpF*, *b*S139C, *b*C21A	This study
pET-atpF3	*atpF*, *b*L65C, *b*C21A	This study
pET-atpEF1	*atpEF*, *b*N2C, *c*V74C, *b*C21A	This study
pET22-atpH-TTG	*atpH* with TTG as start codon	This study
pBAD33 derivatives		
pBAD33	Cm^R, araC, pACYC184 origin	Ref. 24
pBAD33.atp	*atpI′BEFHAGDC*	This study
pBAD33.Δδ	*atpI′BEFH***AGDC*, δY11end	This study
Miscellaneous		
pBR322	Ap^R, Tc^R, pMB1 origin	New England Biolabs
pDF163.b2-c74	Ap^R, pMB1 origin, *atpI′BEFH*, *b*N2C, *c*V74C, *b*C21A	Ref. 25
pFV2	Ap^R, pACYC177 origin, *atpI′BEFHAGDC*, f-MRGSHHHHHHG N-terminally to β	Ref. 26
pMM10	Ap^R, pACYC177 origin, *atpI′BEFHAGDC*, αP280C, γA285C, γK108C, Cys-less, f-MRGSHHHHHHG N-terminally to β	Ref. 27
pSW3	Ap^R, pACYC177 origin, *atpI′BEFHAGDC*, βD380C, γC87, γK108C, Cys-less, f-MRGSHHHHHHG N-terminally to β	Ref. 27
pT7Pol26	Kan^R, *lacI*, T7*gene1*	Ref. 28

F_1. To characterize in more detail the status of *b* present in membranes of Δ*a* and Δδ, nearest neighbor analyses were performed with wild type and mutant membranes containing the amino acid substitution pairs *b*L65C, *b*A92C/αR477C, *b*A92C/βQ351C, or *b*N2C/*c*V74C (Fig. 3); the localization of these residues within F_OF_1 is summarized in Fig. 3*A*. To facilitate reading, the terms wild type (WT), Δ*a*, and Δδ exclusively refer to the mutations leading to partially assembled F_OF_1 complexes independent of the presence or absence of cysteine substitutions. All cysteine pairs used are well characterized to generate disulfide bond formation in wild type with high yield (Fig. 3, *B–E*; compare Refs. 42, 44, and 48) and were applied as indicators for stable interactions between subunits in partially assembled F_OF_1 complexes. The formation of *b*-*b* was comparable in Δ*a* and Δδ with that observed for solely expressed subunit *b* (Fig. 3*B*). In Δ*a*, intense *b*-α and *b*-β heterodimer formation was observed after oxidation with CuP, indicating a proximal localization between b_2 and $\alpha_3\beta_3$ in this partially assembled F_OF_1 complex (Fig. 3, *D* and *E*, *left*). However, no cross-linking could be obtained between subunits *b* and *c* in Δ*a*, suggesting that the

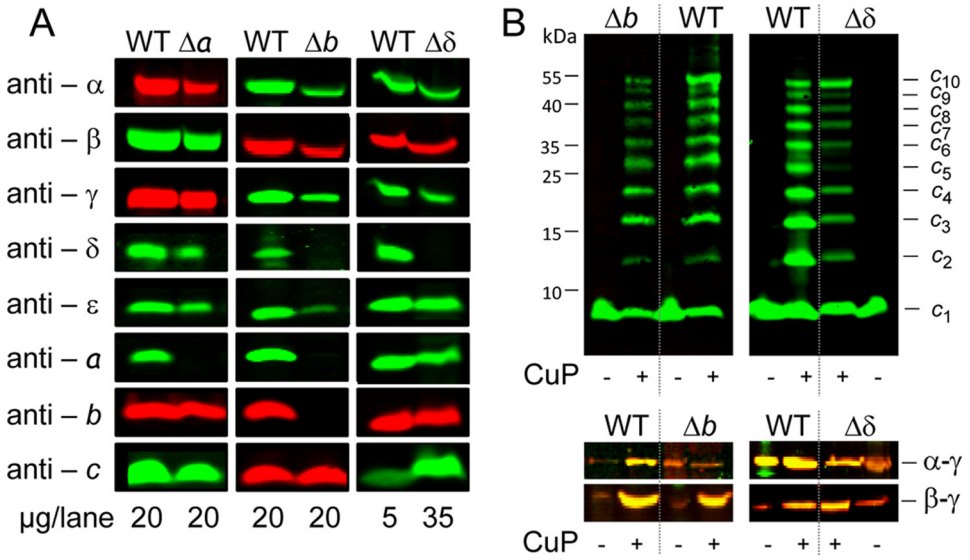

FIGURE 2. **Presence of F_OF_1 subunits in membrane vesicles of single-subunit knock-out mutants Δ*a*, Δ*b*, and Δδ compared with wild type.** *A*, detection of the different F_OF_1 subunits to verify their presence in membrane vesicles. DK8 transformed with pBWU13 (WT), pHB5 (Δ*a*), pBWU13.Δb (Δ*b*), and pBWU13.Δδ (Δδ), respectively, was grown in LB medium with ampicillin and harvested at OD = 0.8–1.0. Membranes were prepared in TMG buffer in the presence of protease inhibitor mix without EDTA and analyzed by immunoblotting. *B*, Cu^{2+}-catalyzed cross-linking within the F_OF_1 core complex $c_{10}\alpha_3\beta_3\gamma\epsilon$ of single-subunit knock-out mutants Δ*b* and Δδ compared with wild type. DK8 transformed with pBWU13 derivatives was grown, membranes were prepared, and after cross-linking with CuP at pH 7.5, proteins were separated by non-reducing SDS-PAGE and analyzed by immunoblotting. *Top*, formation of a cross-linked c_{10} ring using cysteine pair *c*A21C/*c*M65C (WT, pBWU13.NOC; Δ*b*, pJGA5.1; Δδ, pRE3) immunolabeled with monoclonal anti-*c* antibody GDH 9-2A2. Due to an incomplete cross-linking, all intermediate products are visible. *Bottom*, formation of α-γ and β-γ via cysteine substitutions αP280C/γL262C and βD380C/γC87, respectively (α-γ: WT, pBH26.1; Δ*b*, pJGA3; Δδ, pRE8; β-γ: WT, pBH29; Δ*b*, pJGA4; Δδ, pRE10). Immunolabeling was performed with polyclonal mouse (anti-α, anti-β; *green*) and polyclonal rabbit (anti-γ; *red*) antibodies.

right positioning of the amino acid residues of both subunits involved needs the presence of subunit *a* (Fig. 3*C*, *left*). Both cysteine residues are located within terminal regions of the polypeptide chains, which are in general more flexible and, therefore, in most cases a benefit for cross-link formation. However, in this case, a stabilization by subunit *a* seems to be necessary for disulfide bond formation between *b* and *c*, and instead *b*-*b* formation is favored.

In contrast, in Δδ, no cross-linking of subunit *b* to any of its nearest neighbors could be observed, indicating that in the absence of δ, b_2 had no contact with a partially assembled F_OF_1 core complex, at least within the area tested. In general, the ATPase activities observed were within the same range as those measured in the absence of the cysteine substitutions necessary for cross-linking (Table 2).

In the case of *b*-α cross-linking, as a side reaction, an α-α cross-linking was observed, which was analyzed by Brandt *et al.* (48) to be an interenzyme cross-link reaction. Substitution of a cysteine residue in α resulted in incorporation of three thiol groups into F_OF_1. While one thiol group is proximal to the *b* dimer (*b*-α cross-linking in wild type or Δ*a* F_OF_1), the other two, located at the surface of the hexamer, will be freely available for other reactions. Because wild type membranes are rich in F_OF_1, such an intermolecular cross-linking is not unexpected. However, in membranes of mutant Δδ, the amount of F_OF_1 in the membrane was reduced approximately by a factor of 7. Therefore, the probability of interenzyme cross-linking was also reduced, and the amount of α-α varied from experiment to experiment (data not shown).

Taken together, the results revealed that the *b* dimer can be assembled with the core F_OF_1 complex in the absence of subunit *a*, forming a stable complex with interactions in the F_1 part comparable with functional F_OF_1, whereas an integration of b_2 into F_OF_1 is not possible in the absence of subunit δ.

Purification of Partially Assembled F_OF_1 Complexes via N-terminally His_6-tagged Subunit β from Mutants Δ*a and* Δδ—To further characterize the partially assembled core F_OF_1 complex formed in Δ*a* and Δδ, a His_6 tag was fused to the N terminus of subunit β, usually applied to purify ATP synthase complexes from detergent-solubilized wild type membranes (26, 38). For Δ*a* and Δδ, this approach was used to determine which F_OF_1 subunits are stably associated with subunit β. After purification via Ni^{2+}-nitrilotriacetic acid-agarose chromatography, the purified complexes were analyzed by immunoblotting in comparison with their corresponding membranes using antibodies against subunits *b* and γ. Both subunits were in contact with subunit β in wild type F_OF_1 but did not interact with each other (Fig. 4*A*). In membranes, both subunits were present in comparable amounts after adjustment of the amount of membrane protein of Δδ by a factor of 7, as described above (compare Fig. 2*A* and Table 2). After purification of F_OF_1, subunit γ was again present in comparable amounts in both mutants, as expected, without any adjustment. In contrast, for subunit *b*, a different picture emerged; whereas in Δ*a* the amount of *b* was comparable with wild type F_OF_1, subunit *b* was not co-purified and, therefore, was completely missing in the subcomplex purified via His_6-β by affinity chromatography from Δδ. To further characterize the subcomplexes isolated using His_6-β as the bait, immunoblot analyses were carried out for all F_OF_1 subunits (Fig. 4*B*). In Δ*a*, all subunits except *a*, which was knocked out, were present in amounts comparable with wild type, verifying that an F_OF_1-a complex can be stably assembled.

TABLE 2
ATPase activities of *E. coli* strain DK8/pBWU13 and its Δ*a*, Δ*b*, and Δδ derivatives

Strain/plasmid	Description	ATPase activity
		μmol P_i · min^{-1} · mg^{-1}
DK8/pBWU13	WT	1.52
DK8/pHB5	Δ*a*	1.65
DK8/pBWU13.Δδ	Δδ	0.29
DK8/pBWU13.Δb	Δ*b*	0.36
DK8/pBH7	WT His_6-β	1.25
DK8/pBH55.β-His	Δ*a* His_6-β	1.59
DK8/pBH56.β-His	Δδ His_6-β	0.11
DK8/pBH1	WT His_{12}-*a*	1.12
DK8/pBH56.a-His12	Δδ His_{12}-*a*	0.11
DK8/pSTK8	WT *b*L65C	0.85
DK8/pHB17	Δ*a* *b*L65C	1.05
DK8/pRE4	Δδ *b*L65C	0.10
DK8/pKB1.αR477C	WT *b*A92C, αR477C	1.16
DK8/pBH55.bα	Δ*a* *b*A92C, αR477C	1.23
DK8/pRE14	Δδ *b*A92C, αR477C	0.18
DK8/pJPKB.βQ351C	WT *b*A92C, βQ351C	1.16
DK8/pBH55.bβ	Δ*a* *b*A92C, βQ351C	0.75
DK8/pBH56.bβ	Δδ *b*A92C, βQ351C	0.17
DK8/pHB3	WT *b*N2C, *c*V74C	1.09
DK8/pHB15	Δ*a* *b*N2C, *c*V74C	1.04
DK8/pRE2	Δδ *b*N2C, *c*V74C	0.18
DK8/pKB7.aN238C	WT *a*N238C, *b*A13C	0.95
DK8/pSP2.a238/b13	Δδ *a*N238C, *b*A13C	0.18
DK8/pBH152	WT *a*N238C, *b*A13C, *b*E155C	0.68
DK8/pBH152.Δδ	Δδ *a*N238C, *b*A13C, *b*E155C	0.06
DK8/pBH26.1	WT αP280C, γA285C	0.86
DK8/pRE8	Δδ αP280C, γA285C	0.18
DK8/pJGA3	Δ*b* αP280C, γA285C	0.33
DK8/pBH29	WT βD380C, γC87	0.72
DK8/pRE10	Δδ βD380C, γC87	0.24
DK8/pJGA4	Δ*b* βD380C, γC87	0.27
DK8/pBWU13.NOC	WT *c*A21C, *c*M65C	0.82
DK8/pRE3	Δδ *c*A21C, *c*M65C	0.15
DK8/pJGA5.1	Δ*b* *c*A21C, *c*M65C	0.26
DK8/pSTK3	WT *b* Cys-less	1.39
DK8/pBH16	WT *b*Q10C	1.52
DK8/pBH17	WT *b*S139C	1.12
DK8/pBH20.1	WT *b*E155C	0.88

In contrast, in Δδ, subunits δ and *b* could not be detected, and in addition, subunit *a* was only present in extremely low amounts and, therefore, barely visible. The results demonstrate that although subunits *a* and *b* are present in the cytoplasmic membrane of Δδ, they cannot be assembled into F_OF_1 in the absence of subunit δ, as has also been observed for subunit *b* by cross-linking (compare Fig. 3). Nevertheless, a protein complex, which comprises subunits α, β, γ, ϵ, and *c*, could be isolated from Δδ membranes by use of His_6-β as ligand in affinity chromatography, implying the presence of an $c_{10}\alpha_3\beta_3\gamma\epsilon$ subcomplex.

Purification of Partially Assembled F_OF_1 Subcomplexes via N-terminally His_{12}-tagged Subunit a from Mutant Δδ—Accordingly, in the next step, we studied the status of subunit *a* present in the membrane of Δδ by affinity chromatography using a His_{12} tag N-terminally fused to subunit *a* (23, 41). A modified purification protocol was applied to membranes of wild type and Δδ. The immunoblot analysis using anti-*a* and anti-*b* antibodies simultaneously revealed the presence of both subunits in the eluate for wild type and Δδ (Fig. 4*C*). In addition, the eluates obtained were screened for the presence of other F_OF_1 subunits by immunoblotting (Fig. 4*D*). Although from wild type membranes, the entire ATP synthase complex was purified, only subunit *b* could be co-purified from membranes of Δδ using His_{12}-*a* as bait, indicating that a separate subcomplex is formed. Taken together, in the absence of subunit δ, two F_OF_1 subcomplexes are independently present in the cytoplasmic membrane, one comprising subunits α, β, γ, ϵ, and *c* and the other containing the residual subunits *a* and *b*.

Formation of an ab_2 Subcomplex in Membranes of Mutant Δδ—To verify the presence of an independent ab_2 subcomplex in Δδ, we used an experimental set-up in which two cysteine pairs were combined for cross-linking of two different subunit contact areas. As shown in Fig. 5*A* for wild type membranes, in the presence of CuP as oxidant, *b*E155C located in the C-terminal region of subunit *b* was able to generate a *b-b* product, whereas the cysteine pair *b*A13C/*a*N238C located in the transmembrane region of both subunits formed a disulfide bond between subunit *a* and one of the *b* subunits (*b-a*). After combining both cross-linking pairs, an *a-b-b* cross-linked complex was obtained in high yield in the presence of CuP (*b-b*/*b-a*), exhibiting a molecular mass of ~65 kDa, as expected. Due to the presence of the cysteine substitutions, the ATPase activity was reduced by a factor of approximately 2 (Table 2); however, the DCCD sensitivity remained unchanged (78.4% inhibition), indicating a tight coupling between F_1 and F_O in those membranes.

After introducing the corresponding cysteine residues into subunits *a* and *b* of mutant Δδ, the addition of CuP allowed the formation of an *a-b* cross-linking product in the presence of cysteine residues *b*A13C/*a*N238C (Fig. 5*B*) and, furthermore, the formation of a tertiary *a-b-b* product when, in addition, cysteine residue *b*A155C was provided (Fig. 5*C*), suggesting that an ab_2 subcomplex was purified using His_{12}-*a* for affinity chromatography. In each case, *b-b* was observed as byproduct. In summary, membranes of Δδ contained two F_OF_1 subcomplexes, an ab_2 subcomplex and a $c_{10}\alpha_3\beta_3\gamma\epsilon$ subcomplex, both verified by a combination of affinity purification and zero length cross-linking and the latter exhibiting ATPase activity, whereas in membranes of Δ*a*, an F_OF_1 complex lacking only subunit *a* (F_OF_1-a) was assembled, showing ATPase activities comparable with wild type F_OF_1.

Time-delayed in Vivo Assembly of Subunit δ *into Preformed F_OF_1 Subcomplexes Generating a Functional ATP Synthase*—The presence of the two subcomplexes, ab_2 and $\alpha_3\beta_3\gamma\epsilon c_{10}$, in membranes of Δδ, just missing knocked out subunit δ, implies that δ is probably the last subunit being assembled into F_OF_1, as has been suggested by Rak *et al.* (19) for yeast mitochondrial F_OF_1. To answer the question, we applied our time-delayed *in vivo* assembly system (30) for a time-delayed integration of subunit δ into preformed F_OF_1 subcomplexes missing subunit δ.

The experimental design of the time-delayed *in vivo* assembly system is depicted in Fig. 6. After inoculation, P_{araBAD} was induced by arabinose to allow synthesis of F_OF_1 subunits except δ ($F_OF_1-\delta$). During this growth phase, the *lac* operator-controlled promoters were repressed (compare Fig. 8*B*) due to pre-

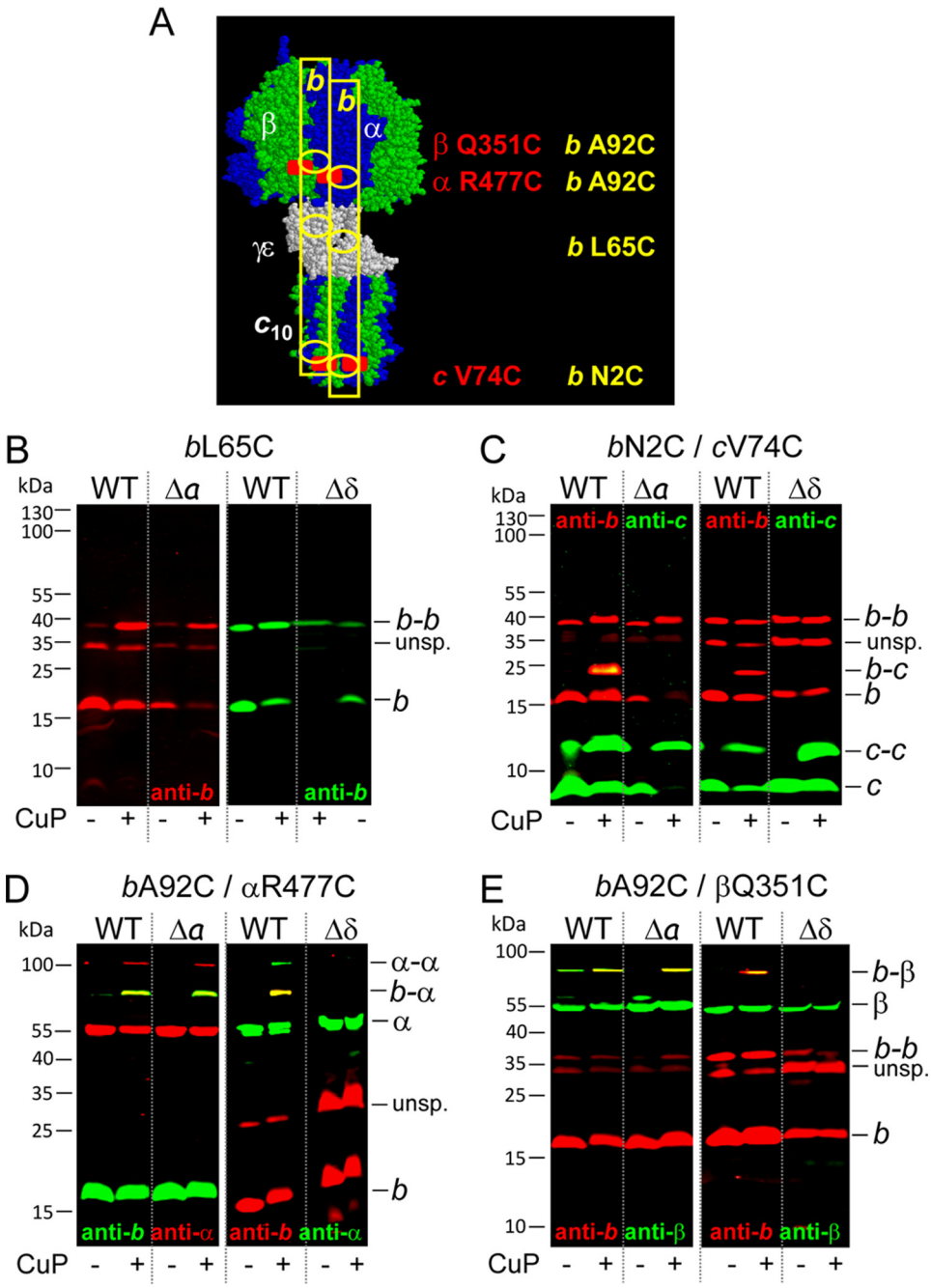

FIGURE 3. **Cu^{2+}-catalyzed cross-linking of subunit *b* to subunit α, β, or *c* in membranes of knock-out mutants Δ*a* and Δδ compared with wild type.** DK8 transformed with pBWU13 derivatives was grown, and membranes were prepared as described in the legend of Fig. 2. Membranes of wild type, Δ*a*, and Δδ, containing F_OF_1 subunits individually substituted with cysteines, were separated after cross-linking with CuP at pH 7.5 by non-reducing SDS-PAGE and analyzed by immunoblotting. *A*, structural homology model of $c_{10}\alpha_3\beta_3\gamma\epsilon$ of *E. coli* ATP synthase. The model is composed of several partial structures combined with biochemical data as described in detail by Junge *et al.* (1) and drawn by RasMol version 2.7.2.1.1 to mark the positions of the cross-linking pairs used, with b_2 illustrated as *yellow rectangles*. *B*, formation of *b* dimer via cysteine substitution *b*L65C (WT, pSTK8; Δ*a*, pHB17; Δδ, pRE4). *C*, cross-linking between subunits *b* and *c* using cysteine pair *b*N2C/*c*V74C (WT, pHB3; Δ*a*, pHB15; Δδ, pRE2). *D*, cross-linking between subunits *b* and α using cysteine pair *b*A92C/αR477C (WT, pKB1.αR477C; Δ*a*, pBH55.bα; Δδ, pRE14). *E*, cross-linking between subunits *b* and β via cysteine pair *b*A92C/βQ351C (WT, pJPKB.βQ351C; Δ*a*, pBH55.bβ; Δδ, pBH56.bβ). *B–E*, *left*, WT, 20 μg/lane; Δ*a*, 20 μg/lane. *B–E*, *right*, WT, 5 μg/lane; Δδ, 35 μg/lane. *unsp.*, unspecific.

incubation of the medium with β-galactosidase for removal of residual lactose and the use of TTG as a start codon for *atpH*. At OD = 0.3, P_{araBAD} was repressed by the simultaneous addition of the catabolite repressor glucose and the anti-inducer D-fucose, a non-metabolizable analog of L-arabinose, and, after further growth for 20 min, nearly all *atp* mRNA present in the cell was degraded (see below). Due to this time delay, the *de novo* biosynthesis of F_OF_1 subunits was completely prevented. Subsequently, IPTG induction of *lac* operator-controlled promoters enabled the individual synthesis of subunit δ, which might be assembled together with the preformed subcomplexes ab_2 and $c_{10}\alpha_3\beta_3\gamma\epsilon$ ($F_OF_1-\delta+\delta$) to generate functional F_OF_1.

The stability of both subcomplexes formed was controlled by immunoblotting applying antibodies against subunits *a*, *b*, α, and γ to analyze both subcomplexes individually (Fig. 7*A*). Cells of $F_OF_1-\delta$ were grown to OD = 0.3 in the presence of arabinose

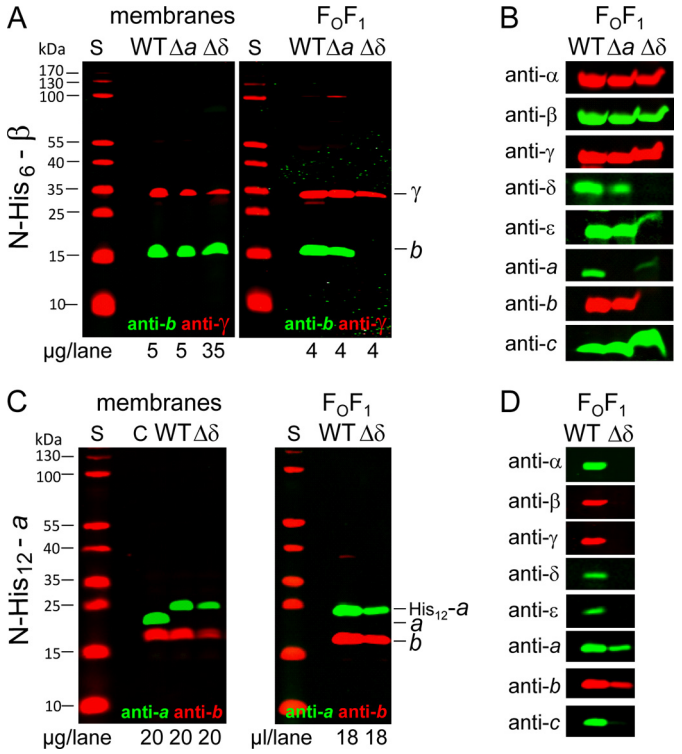

FIGURE 4. **Purification of partially assembled F_OF_1 of mutants Δ*a* and Δδ by affinity chromatography in comparison with wild type.** *A* and *C*, comparison of membranes and purified F_OF_1 complexes. *B* and *D*, detection of the different F_OF_1 subunits to verify their presence in the complexes purified. DK8 transformed with pBWU13 derivatives was grown as described in the legend of Fig. 2. Membranes were prepared and solubilized, and F_OF_1 complexes were purified by affinity chromatography via a His_6 tag (*A* and *B*) present N-terminal to subunit β (WT, pBH7; Δ*a*, pBH55.β-His; Δδ, pBH56.β-His) or a His_{12} tag (*C* and *D*) fused to the N terminus of subunit *a* (WT, pBH1; Δδ, pBH56.a-His12). Membranes and purified F_OF_1 were analyzed by immunoblotting. *S*, molecular mass standard; *C*, subunits *a* and *b* detected in membranes of DK8/pBWU13.

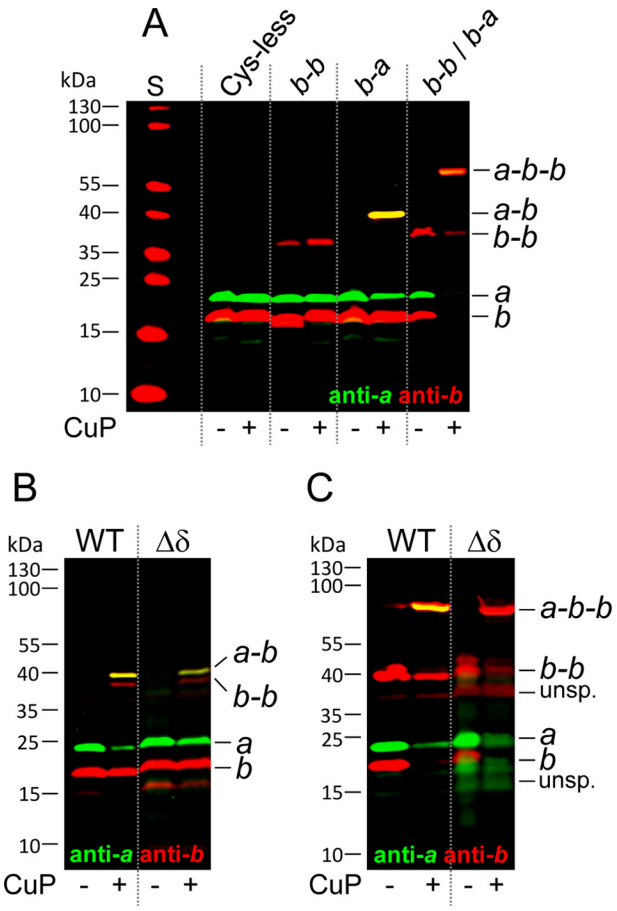

FIGURE 5. **Cross-linking between subunits *a* and *b* in membranes of Δδ compared with wild type.** Cell growth, membrane preparation, and cross-linking at pH 8.2 were performed as described in the legend of Fig. 3. Membranes were separated by non-reducing SDS-PAGE and analyzed by immunoblotting. *A*, generation of an *a-b-b* subcomplex by combining cross-linking pairs *b*A13C/*a*N238C and *b*E155C (Cys-less, pSTK3; *b-b*, pBH20.1; *b-a*, pKB7.aN238C; *b-b*/*b-a*, pBH152) using 20 μg protein/lane. *B*, cross-linking between subunits *b* and *a* using the cysteine pair *b*A13C/*a*N238C in mutant Δδ (WT, pKB7.aN238C; Δδ, pSP2.a238/b13). *C*, formation of a cross-linked *a-b-b* subcomplex in mutant Δδ (WT, pBH152; Δδ, pBH152.Δδ) using different amounts of protein (WT, 5 μg/lane; Δδ, 35 μg/lane). *S*, molecular mass standard; *unsp.*, unspecific.

(Ara) before the addition of glucose and D-fucose (Glu/Fuc), and in defined time intervals, samples were taken for analysis of F_OF_1 subunits in cell lysates. Whereas the amount of α and γ was stable over a period of at least 60 min, the immunodetection of *a* and *b* revealed a continuous degradation of ab_2, starting at the latest after 30 min, and implies that the ab_2 subcomplex is more susceptible to degradation by proteases than the core complex $c_{10}\alpha_3\beta_3\gamma\epsilon$. In parallel, the decomposition of the *atp* mRNA was controlled by rt-RT-PCR, revealing a complete degradation 15 min after the addition of Glu/Fuc (Fig. 7*B*). Therefore, the delay time for the degradation of *atp* mRNA, being simultaneously the starting point for the synthesis of δ, was set to 20 min.

Different cell batches of $F_OF_1-\delta$ were grown, each with the additives added at the time points addressed in Fig. 6. As a control, samples expressing wild type F_OF_1 were handled correspondingly. Under Ara-induced conditions, *atp* mRNA was present within the cells, as shown by rt-RT-PCR (Fig. 8*A*), although the amount was reduced in $F_OF_1-\delta$ by a factor of approximately 3 compared with wild type. In samples containing Glu/Fuc independent of the presence of Ara, *atp* mRNA was almost completely absent (0.3–2%), revealing that the synthesis of F_OF_1 subunits is prohibited.

Immunoblotting using antibodies against subunits *b* and γ as representatives of the two subcomplexes formed also revealed a reduction for $F_OF_1-\delta$ compared with F_OF_1 under Ara-induced conditions (Fig. 8*B*). In the presence of Glu/Fuc but in the absence of Ara, no F_OF_1 subunits were detectable in $F_OF_1-\delta$, whereas extremely low amounts could be observed in wild type F_OF_1, which were quantitated to be below 2% by determining ATPase activity (Fig. 8*C*) but remained below the detection limit for ATP-driven H^+ translocation (Fig. 8*D*). Samples induced with Ara and subsequently repressed by Glu/Fuc showed reduced but significant signals by immunolabeling, and again the ATPase activities observed correlated very well (Fig. 8, *B* and *C*). In addition, the extent of subunit degradation after repression with Glu/Fuc (in total for 80 min) was comparable with that observed in Fig. 7*A*. Subunit δ was not detectable in membranes of $F_OF_1-\delta$; however, after expression of *atpH*, it was overproduced beyond stoichiometric amounts ($F_OF_1-\delta+\delta$; Fig. 8*B*). Importantly, a stabilizing effect, especially on subunit *b*, could be observed due to induction of *atpH* expression, whereas the

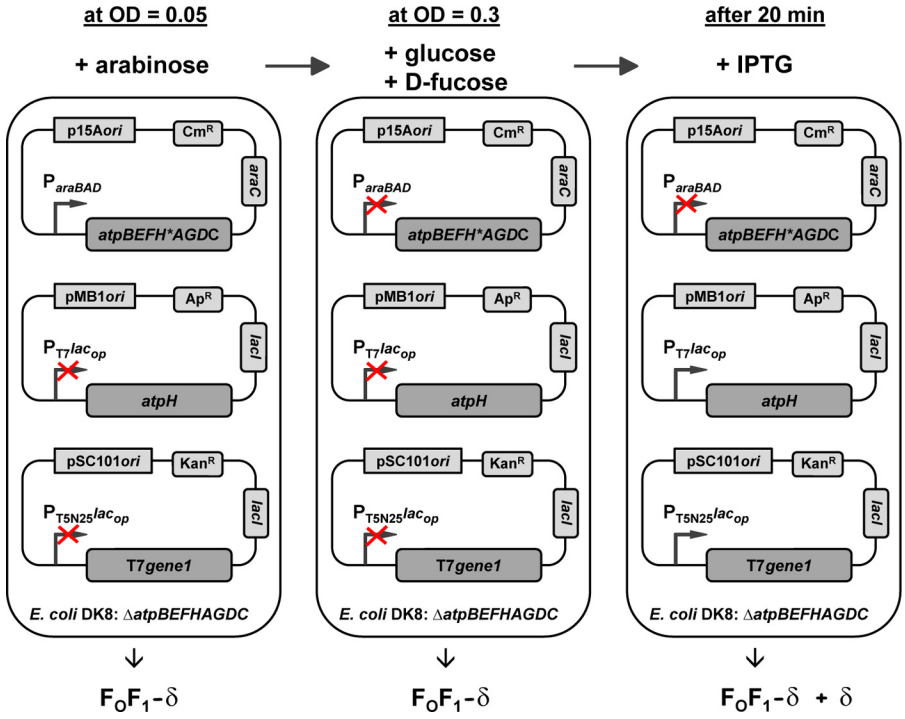

FIGURE 6. **Design of the time-delayed *in vivo* assembly system and its different states during cell growth.** Δ*atpB-C* strain DK8 was transformed with three plasmids bearing different resistance genes and different origins to gain compatibility: (i) a pBAD33 derivative (p15A *ori*; Cm^R) with structural genes of the *atp* operon carrying an early stop codon (δY11end) in *atpH* (*atpBEFH*AGDC*) under control of P_{araBAD}; (ii) a pET-22b derivative (pMB1 *ori*, Ap^R) carrying the *atpH* gene under control of the IPTG-inducible $T7_{lac}$ promoter using the weak start codon TTG for *atpH*; (iii) a pSC101 derivative (Kan^R) containing T7 *gene1* under control of the IPTG-inducible $T5N25_{lac}$ promoter, encoding the RNA polymerase specific for promoters of phage T7. *Left*, cells were inoculated with OD = 0.05; P_{araBAD} was induced by arabinose to allow expression of the *atpBEFH*AGDC* genes, and the F_OF_1 subunits except for subunit δ ($F_OF_1-\delta$) were synthesized. During this growth phase, the *lac* operator-controlled promoters are completely repressed. *Middle*, at OD = 0.3, P_{araBAD} is repressed by the simultaneous addition of glucose and D-fucose, and after further growth for 20 min, the *atp* mRNA present within the cell is completely degraded. Due to this time delay, the *de novo* biosynthesis of F_OF_1 subunits is prevented. *Right*, time-delayed IPTG induction of *lac* operator-controlled T7 and T5N25 promoters for 1 h enables the synthesis of subunit δ assembling together with the preformed F_OF_1 subcomplexes ab_2 and $c_{10}\alpha_3\beta_3\gamma\epsilon$ ($F_OF_1-\delta+\delta$), a functional F_OF_1 complex. *Red cross*, repressed or uninduced state of promoters.

amount of γ as well as membrane-bound ATPase activity remained unchanged (Fig. 8, *B* and *C*). After repression of *atp* transcription by Glu/Fuc, degradation of subunits was observed for F_OF_1 as well as $F_OF_1-\delta+\delta$. Nevertheless, in the absence of subunit δ ($F_OF_1-\delta$), the degradation of *b* is increased, supporting the notion that δ protects the ab_2 subcomplex against proteolytic digestion probably by its integration into the holoenzyme, whereas the stability of the $c_{10}\alpha_3\beta_3\gamma\epsilon$ remained unaffected.

The acidification of the lumen of membrane vesicles by ATP-driven H^+ translocation was measured using ACMA as a pH-sensitive dye and applied to determine the assembly of a functional F_OF_1 complex from subcomplexes (Fig. 8*D*). Under Ara-induced conditions, the fluorescence quenching rates obtained for F_OF_1 were within the range expected (40, 49). After the addition of Glu/Fuc in the presence of Ara, the quenching rate was only slightly decreased, although the ATPase activity revealed that the amount of F_OF_1 in the membrane had been reduced to one-third, a discrepancy only at first glance that is probably due to a less dense protein packing within the membrane and, therefore, a significantly decreased membrane proton permeability (23, 50), leading to a stronger acidification of the vesicle lumen. Under repressed conditions, no H^+ transport could be observed for F_OF_1 as well as $F_OF_1-\delta$, although H^+ pumping via the respiratory chain with NADH as substrate revealed intactness of the vesicles (data not shown), indicating a tight repression of P_{araBAD} by Glu/Fuc. In contrast, $F_OF_1-\delta$ showed extremely low H^+ pumping rates (below 3%) in the presence of Ara. However, these rates were independent of the presence/absence of Glu/Fuc, implying that now and then spontaneously an H^+-conducting unit could be formed from the two individual subcomplexes containing subunits *a* and *c*, an assumption corroborated by the complete absence of ATP-driven H^+ transport in otherwise identical experiments performed with F_OF_1-a (30); an observation that requires further investigations to clarify whether subunit δ increases the affinity of ab_2 for the F_OF_1 core complex or whether it changes the conformation of subunit *a* to an active one. However, after synthesis of subunit δ ($F_OF_1-\delta+\delta$) the quenching rate increased to 21.4%, demonstrating that functional F_OF_1 was assembled (Fig. 8*D*). The rate obtained fits well with the corresponding ATPase activity, and furthermore, both values are in good correlation with the activities of wild type F_OF_1 (in the presence of Ara and Glu/Fuc), indicating that both enzyme complexes independent of their assembly pathway exhibit comparable ATPase activities. Furthermore, ATP-driven H^+ transport was completely abolished after preincubation of F_OF_1 as well as $F_OF_1-\delta+\delta$ membranes with DCCD (data not shown). DCCD, which modifies specifically the protonated carboxyl groups of Asp-61 of subunit *c* at pH 8.0, inhibits the rotation of the c_{10} ring and, thereby, H^+ translocation. Taken together, a functional F_OF_1 complex was assembled from subcomplexes ab_2 and $c_{10}\alpha_3\beta_3\gamma\epsilon$ by time-delayed synthesis of subunit δ.

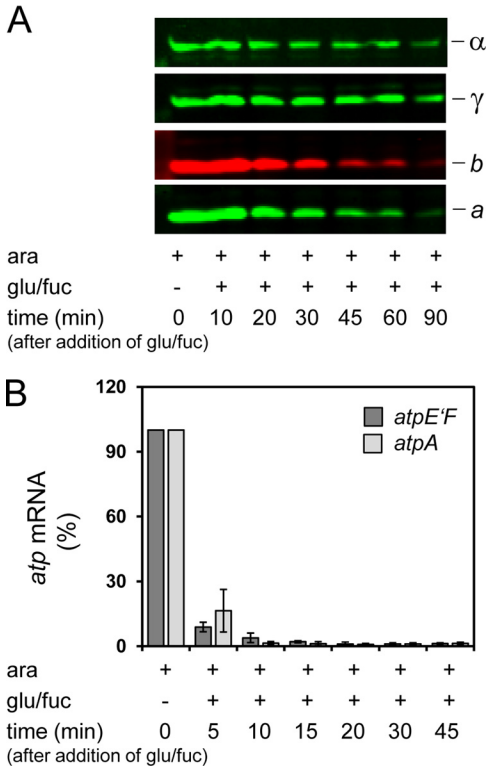

FIGURE 7. **Stability of $F_OF_1-\delta$ (*A*) and degradation of *atp* mRNA (*B*) after repression of P_{araBAD} controlling expression of *atpBEFH*AGDC*.** DK8 carrying plasmids pBAD33.Δδ, pET22.atpH-TTG and pT7POL26 ($F_OF_1-\delta$) was grown as described under "Experimental Procedures." At each time point indicated, cells were harvested for immunoblot analysis (*A*) and isolation of RNA (*B*). *A*, stability of $F_OF_1-\delta$. After resuspension of cell lysates in sample loading buffer, cells were incubated for 5 min at 99 °C. The amount of cell extract (20 μg/lane) was calculated according to the determination of Neidhardt *et al.* (34) that 160 μg of protein is present per ml of growth medium at OD = 1. Proteins were separated by SDS-PAGE and detected by immunolabeling as indicated. *B*, degradation of *atp* mRNA. rt-RT-PCR was performed using primer pairs *atpE'F* (*dark gray*) and *atpA* (*light gray*). The amount of *atp* mRNA present in the F_OF_1 sample grown with Ara was set to 100%. *Error bars*, S.E.

DISCUSSION

Generation of the H^+-translocating Unit—The F_O complex of *E. coli* ATP synthase is composed of subunits *a*, *b*, and *c* present as ab_2c_{10}. Wild type membranes depleted of F_1 revealed an F_O complex functional in H^+ conduction as well as rebinding of F_1 (40, 49). Furthermore, purification of F_O subunits and reconstitution into liposomes revealed the same characteristics (51, 52). In contrast, after synthesis of F_O subunits in the absence of F_1, only low levels of proton permeability were observed in membranes as well as after reconstitution into liposomes, implying a dependence on F_1 for the proton translocation by F_O (53, 54), although the additional presence of subunit δ enhances the proton conduction through F_O (55, 56).

Our results indicate that subunit δ is the key player in generating the functional H^+-translocating unit composed of ac_{10}. The position of b_2 in F_OF_1 is restricted by its specific interactions with subunits *a* and δ at both terminal regions. The characterization of partially assembled F_OF_1 in Δ*a* and Δδ, however, revealed that both interactions do not influence each other; the binding of *a* and δ to b_2 are two unrelated processes apparently without major conformational changes. Whereas in Δ*a*, b_2 interacts with δ, thereby enabling its integration into F_OF_1, in Δδ, a specific ab_2 subcomplex is formed by specific interaction with subunit *a*. Moreover, time-delayed binding of the second interaction partner (subunit δ (Fig. 8) or subunit *a* (30)) is possible without any preassigned assembly sequence, leading to the formation of a functional F_OF_1 complex in each case. As a consequence, it can be concluded that subunit δ is functioning as a clamp to induce a first contact between ab_2 and c_{10} (via $\alpha_3\beta_3\gamma\epsilon$) to generate the H^+-conducting unit within the membrane because the exclusive presence of both subcomplexes in Δδ is not sufficient to constitute an open H^+ channel. By this arrangement, two important characteristics of F_OF_1 are respected. First, an intermediate assembly product exhibiting uncontrolled H^+ conduction is avoided, which would lead to a breakdown of the proton motive force and, therefore, be lethal for the cell. Instead, it is guaranteed that an open H^+ channel is concomitantly assembled within a coupled F_OF_1 complex, thereby preventing membrane proton permeability. Second, due to the rotation of the c_{10} ring *versus* the stator part ab_2, it is essential for function that the affinity between stator and rotor subunits in F_O is low. In addition, the recent 9.7 Å cryoelectron microscopy structure of the A-type ATP synthase of *Thermus thermophilus* (57) revealed a surprisingly small contact area between the rotor ring and the I protein (equivalent to subunit *a* of F-type ATP synthases). This low affinity is elegantly bypassed by subunit δ holding both complexes of F_O, ab_2 as well as c_{10} (via $\alpha_3\beta_3\gamma\epsilon$), in position, with b_2 providing the necessary stiffness.

Nonetheless, as described above, once the F_O complex has been generated, a depletion of F_1 is possible without major changes in its H^+-conducting capabilities, indicating that the first contact between ab_2 and c_{10} enabled by δ triggers a kind of induced fit within subunits *a* and *c* that later on facilitates binding between F_O subunits in the absence of F_1. However, whether subunit δ simply increases the affinity of ab_2 for the rest of the complex or whether it changes the conformation of F_O to an active one, as suggested previously (55, 56), remains to be solved in further investigations.

Assembly of E. coli ATP Synthase from Subcomplexes—Our results support the notion that *E. coli* F_OF_1 is assembled from different subcomplexes (summarized in Fig. 9). The formation of b_2 is independent of the presence of other F_OF_1 subunits, as shown by zero length cross-linking. With the same experimental design, it has recently been demonstrated that the c_{10} ring is also stably organized in the absence of other F_OF_1 subunits (4). Furthermore, a simultaneous but exclusive expression of subunits *b* and *c* in stoichiometric amounts allowed no *b-c* cross-link formation using a contact site characterized for wild type F_OF_1 (25). Although both subunits are overexpressed, no interaction between subunits *b* and *c* could be observed in the absence of other F_OF_1 subunits, which is in contrast to the model for assembly of *E. coli* F_OF_1 proposing a b_2c_{10} subcomplex as an intermediate product (59, 60) but in accordance with models proposed for yeast mitochondrial ATP synthase (19, 58, 61).

Characterization of Δδ and Δ*b* revealed the presence of the membrane-bound core complex $c_{10}\alpha_3\beta_3\gamma\epsilon$ possessing ATPase activity with rates comparable with wild type in relation to the amount of protein present. Furthermore, due to the absence of subunits *a*, *b*, and δ in Δ*b*, it can be concluded that core complex formation occurs independently of other subcomplexes. Until now, only little experimental data regarding the order of the

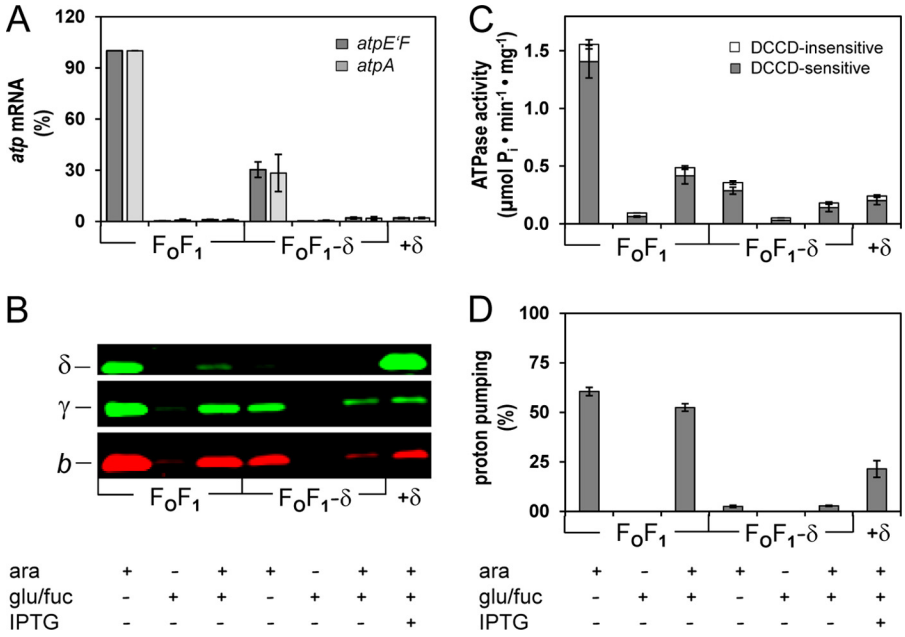

FIGURE 8. **Time-delayed *in vivo* assembly system of subunit δ into preformed F_OF_1 subcomplexes yielding functional F_OF_1.** *A–D*, DK8 carrying plasmids pBAD33.atp, pET-22b, and pT7POL26 (F_OF_1) or pBAD33.Δδ, pET22-atpH-TTG, and pT7POL26 ($F_OF_1-\delta$; $F_OF_1-\delta+\delta$) was grown as described under "Experimental Procedures." Seven independent cell batches were prepared in parallel containing the additives indicated. The data represent average values of three independent measurements. *A*, level of *atp* mRNA. The amount of *atp* mRNA was determined via rt-RT-PCR using primer pairs *atpE'F* (*dark gray*) and *atpA* (*light gray*). The amount of *atp* mRNA present in the F_OF_1 sample grown with Ara was set to 100%. *B*, immunoblot analysis of membrane vesicles (20 μg of protein/lane) as indicated. *C*, ATPase activity of membrane vesicles. *Gray* and *white* portions of the *bars* represent DCCD-sensitive and DCCD-insensitive fractions of ATP hydrolysis, respectively. *D*, ATP-driven proton translocation of membrane vesicles. The relative magnitude of ACMA fluorescence quenching induced by ATP is shown. *Error bars*, S.E.

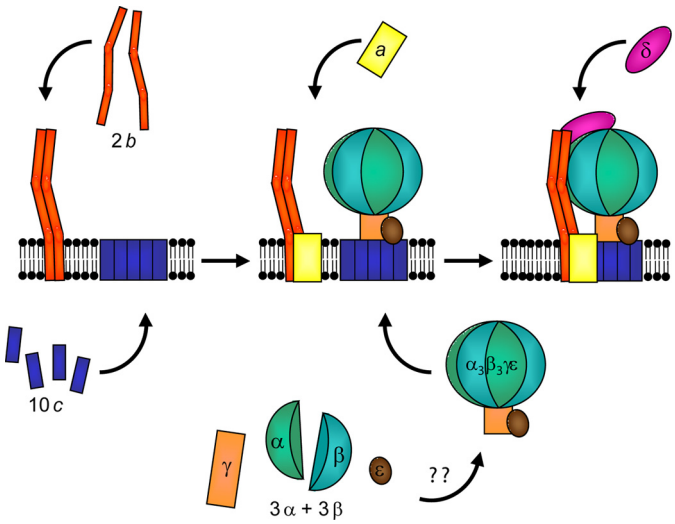

FIGURE 9. **Model for the assembly of *E. coli* ATP synthase.** The assembled c_{10} ring and b_2 are independently present in cytoplasmic membranes. Formation of $\alpha_3\beta_3\gamma\epsilon$ is not known in detail for *E. coli*. For F_OF_1 from yeast mitochondria, it has been proposed that two subcomplexes, $\alpha_3\beta_3$ hexamer and $\gamma\epsilon$, are assembled, which combine to form $\alpha_3\beta_3\gamma\epsilon$, before it subsequently binds to the membrane-bound c_{10} ring (58, 19). The membrane insertion of subunit *a* is interdependent on the presence of *b* and *c*. Integration of b_2 into the complex is dependent on subunit δ, whereas binding of *a* as well as δ to b_2 possibly has no preferred sequence.

assembly of the *E. coli* F_1 part have been available. However, *in vitro* reconstitution experiments (13, 62, 63) support an assembly in the cytoplasm prior to its binding to the *c* ring comparable with that described for yeast mitochondrial F_1 (19, 64, 65). Therefore, an assembly of the F_OF_1 core complex from two individual subcomplexes c_{10} and $\alpha_3\beta_3\gamma\epsilon$ is proposed, with $\alpha_3\beta_3\gamma$ forming the minimal unit exhibiting ATPase activities (12, 62, 66) and subunit ε being necessary for a stable binding to the membrane via c_{10} (63, 67). Preliminary experiments on chromosomally expressed ATP synthase containing His_6-β enabled the purification of subunits α, β, γ, and ε exhibiting ATPase activity.[7]

In mutant Δδ, a separate ab_2 subcomplex is present in the membrane in addition to the ATP-hydrolyzing F_OF_1 core complex. Furthermore, time-delayed synthesis of subunit δ enabled a subsequent assembly of functional ATP synthase, supporting the notion that both subcomplexes are present as native assembly intermediates. In addition, a reduction in synthesis of subunit *c* due to a point mutation in the ribosome binding site of *atpE* revealed the presence of free ab_2 subcomplexes that can be reconstituted in liposomes with subunit *c* after purification to form F_O complexes functional in passive H^+ translocation as well as F_1 binding (23). Due to the plasmid-encoded overexpression of F_OF_1 subunits, free excess subunits are inevitably present in the cell, and therefore, the assembly of active F_OF_1 complexes from these isolated subunits during time-delayed synthesis of subunit δ is at least conceivable. However, the observation that the amount of subunit γ present in the membrane as well as the membrane-bound ATPase activity remained unchanged after time-delayed expression of subunit δ revealed that ab_2 as well as $c_{10}\alpha_3\beta_3\gamma\epsilon$ are true assembly intermediates instead of dead end products of incomplete assembly.

Last Subunit Being Assembled into F_OF_1—Whereas in Δ*a*, a single subcomplex just missing subunit *a* is assembled, in Δδ, two subcomplexes, ab_2 and $c_{10}\alpha_3\beta_3\gamma\epsilon$, are present in the mem-

[7] G. Deckers-Hebestreit, unpublished observation.

brane. Furthermore, in both cases, a time-delayed synthesis of the missing subunit enabled the formation of functional ATP synthase, suggesting that each subunit can be assembled as the last subunit into preformed subcomplexes. Comparable results have been described for *Bacillus* PS3 as well as mitochondrial F_OF_1. Thermophilic *Bacillus* PS3 F_OF_1 lacking subunit *a* (F_OF_1-a) can be isolated in stable form from *E. coli* membranes, and after co-reconstitution with independently purified or cell-free synthesized subunit *a*, both components form a functional enzyme complex in liposomes (68, 69). In addition, from human ρ^0 cells, a stable F_OF_1 complex lacking subunits *a* (Atp6p) and A6L (an additional subunit not present in bacterial F_OF_1) was purified (70). On the other hand, the data of Rak *et al.* (19) revealed that F_OF_1 is assembled in a modular way from at least three different modules, F_1, the *c* ring, and a stator subcomplex. No information is given, however, for the assembly of OSCP (homologous to bacterial δ) into F_OF_1, although it has been deduced that OSCP might may be last subunit being assembled.

This seems to be contradictory at first sight; however, it is probably due to the manipulative conditions applied. In each case, the use of mutants provokes an arrest in the assembly pathway at a certain point, whereas in wild type cells, all subunits are nearly isochronously at hand by their simultaneous translation from polycistronic mRNA (15, 71). Apparently, subunit *a* as well as subunit δ could bind to preformed b_2, probably simultaneously due to their autonomous interaction, therefore implying that *in vivo* a subcomplex of $ab_2\delta$ is formed prior to its binding to $c_{10}\alpha_3\beta_3\gamma\epsilon$. This is further supported by the observation that in Δ*b* in addition to *b*, also subunits *a* and δ were absent. *In vitro* studies with purified subunit δ and the hydrophilic part of subunit *b* (comprising amino acid residues 34–156) revealed the formation of a $b_2\delta$ complex (72). On the other hand, subunit δ is highly susceptible to proteolytic digestion and, therefore, rapidly degraded in most single-subunit knockout mutants producing partially assembled F_OF_1 complexes.[7] A proteolytic fragment of subunit δ comprising amino acid residues 1–134 has been characterized (73), although the corresponding protease has not yet been identified. In addition, in the absence of subunit δ, ab_2 as well as $\alpha_3\beta_3\gamma\epsilon$ were also degraded by proteases in appreciable amounts. Certainly, this rapid turnover indicates a tight regulation of δ and underlines its importance in generating functional F_OF_1. Whether δ makes the first contact with its C-terminal region with b_2 (74), forming an $ab_2\delta$ subcomplex, or whether it is first bound with its N-terminal region to the F_OF_1 core complex via subunit α (13, 32), forming a $c_{10}\alpha_3\beta_3\gamma\delta\epsilon$ subcomplex, is the next question to be investigated.

Acknowledgments—We are grateful to Drs. S. D. Dunn (University of Western Ontario), S. B. Vik (Southern Methodist University), R. H. Fillingame (University of Wisconsin Medical School), R. D. Simoni (Stanford University), and S. Engelbrecht (University of Osnabrück) for kindly providing antibodies and plasmids; S. Konrad, J. Garrelfs, and H. Brookman for aid in generating some of the plasmids; and Drs. K. Altendorf and J.-C. Greie for critical reading of the manuscript.

REFERENCES

1. Junge, W., Sielaff, H., and Engelbrecht, S. (2009) Torque generation and elastic power transmission in the rotary F_OF_1-ATPase. *Nature* **459,** 364–370
2. von Ballmoos, C., Wiedenmann, A., and Dimroth, P. (2009) Essentials for ATP synthesis by F_1F_O ATP synthases. *Annu. Rev. Biochem.* **78,** 649–672
3. van der Laan, M., Bechtluft, P., Kol, S., Nouwen, N., and Driessen, A. J. (2004) F_OF_1 ATP synthase subunit *c* is a substrate of the novel YidC pathway for membrane protein biogenesis. *J. Cell Biol.* **165,** 213–222
4. Ballhausen, B., Altendorf, K., and Deckers-Hebestreit, G. (2009) Constant c_{10} ring stoichiometry in the *Escherichia coli* ATP synthase analyzed by cross-linking. *J. Bacteriol.* **191,** 2400–2404
5. Suzuki, T., Ozaki, Y., Sone, N., Feniouk, B. A., and Yoshida, M. (2007) The product of *uncI* gene in F_1F_O-ATP synthase operon plays a chaperone-like role to assist *c*-ring assembly. *Proc. Natl. Acad. Sci. U.S.A.* **104,** 20776–20781
6. Brandt, K., Müller, D. B., Hoffmann, J., Hübert, C., Brutschy, B., Deckers-Hebestreit, G., and Müller, V. (2013) Functional production of the Na^+ F_1F_O ATP synthase from *Acetobacterium woodii* in *Escherichia coli* requires the native AtpI. *J. Bioenerg. Biomembr.* **45,** 15–23
7. Liu, J., Hicks, D. B., and Krulwich, T. A. (2013) Roles of AtpI and two YidC-type proteins from alkaliphilic *Bacillus pseudofirmus* OF4 in ATP synthase assembly and nonfermentative growth. *J. Bacteriol.* **195,** 220–230
8. Kol, S., Majczak, W., Heerlien, R., van der Berg, J. P., Nouwen, N., and Driessen, A. J. (2009) Subunit *a* of the F_1F_O ATP synthase requires YidC and SecYEG for membrane insertion. *J. Mol. Biol.* **390,** 893–901
9. Yi, L., Jiang, F., Chen, M., Cain, B., Bolhuis, A., and Dalbey, R. E. (2003) YidC is strictly required for membrane insertion of subunits *a* and *c* of the F_1F_O ATP synthase and SecE of the SecYEG translocase. *Biochemistry* **42,** 10537–10544
10. Yi, L., Celebi, N., Chen, M., and Dalbey, R. E. (2004) Sec/SRP requirements and energetics of membrane insertion of subunits *a*, *b*, and *c* of the *Escherichia coli* F_1F_O ATP synthase. *J. Biol. Chem.* **279,** 39260–39267
11. Hermolin, J., and Fillingame, R. H. (1995) Assembly of F_O sector of *Escherichia coli* H^+ ATP synthase. Interdependence of subunit insertion into the membrane. *J. Biol. Chem.* **270,** 2815–2817
12. Koebmann, B. J., Westerhoff, H. V., Snoep, J. L., Nilsson, D., and Jensen, P. R. (2002) The glycolytic flux in *Escherichia coli* is controlled by the demand for ATP. *J. Bacteriol.* **184,** 3909–3916
13. Senior, A. E., Muharemagić, A., and Wilke-Mounts, S. (2006) Assembly of the stator in *Escherichia coli* ATP synthase. Complexation of α subunit with other F_1 subunits is prerequisite for δ subunit binding to the N-terminal region of α. *Biochemistry* **45,** 15893–15902
14. Pati, S., DiSilvestre, D., and Brusilow, W. S. (1992) Regulation of the *Escherichia coli uncH* gene by mRNA secondary structure and translational coupling. *Mol. Microbiol.* **6,** 3559–3566
15. McCarthy, J. E. (1988) Expression of the *unc* genes in *Escherichia coli*. *J. Bioenerg. Biomembr.* **20,** 19–39
16. Walker, J. E., and Cozens, A. L. (1986) Evolution of ATP synthase. *Chem. Scripta* **26B,** 263–272
17. Gomis-Rüth, F. X., Moncalián, G., Pérez-Luque, R., González, A., Cabezón, E., de la Cruz, F., and Coll, M. (2001) The bacterial conjugation protein TrwB resembles ring helicases and F_1-ATPase. *Nature* **409,** 637–641
18. Mulkidjanian, A. Y., Makarova, K. S., Galperin, M. Y., and Koonin, E. V. (2007) Inventing the dynamo machine. The evolution of the F-type and V-type ATPases. *Nat. Rev. Microbiol.* **5,** 892–899
19. Rak, M., Gokova, S., and Tzagoloff, A. (2011) Modular assembly of yeast mitochondrial ATP synthase. *EMBO J.* **30,** 920–930
20. Klionsky, D. J., Brusilow, W. S., and Simoni, R. D. (1984) *In vivo* evidence for the role of the ϵ subunit as an inhibitor of the proton-translocating ATPase of *Escherichia coli*. *J. Bacteriol.* **160,** 1055–1060
21. Moriyama, Y., Iwamoto, A., Hanada, H., Maeda, M., and Futai, M. (1991) One-step purification of *Escherichia coli* H^+-ATPase (F_OF_1) and its reconstitution into liposomes with neurotransmitter transporters. *J. Biol. Chem.* **266,** 22141–22146

22. Krebstakies, T., Zimmermann, B., Gräber, P., Altendorf, K., Börsch, M., and Greie, J. (2005) Both rotor and stator subunits are necessary for efficient binding of F_1 to F_O in functionally assembled *Escherichia coli* ATP synthase. *J. Biol. Chem.* **280,** 33338–33345
23. Krebstakies, T., Aldag, I., Altendorf, K., Greie, J.-C., and Deckers-Hebestreit, G. (2008) The stoichiometry of subunit *c* of *Escherichia coli* ATP synthase is independent of its rate of synthesis. *Biochemistry* **47,** 6907–6916
24. Guzman, L. M., Belin, D., Carson, M. J., and Beckwith, J. (1995) Tight regulation, modulation, and high-level expression by vectors containing the arabinose P_{BAD} promoter. *J. Bacteriol.* **177,** 4121–4130
25. Jones, P. C., Hermolin, J., Jiang, W., and Fillingame, R. H. (2000) Insights into the rotary catalytic mechanism of F_OF_1 ATP synthase from the cross-linking of subunits *b* and *c* in the *Escherichia coli* enzyme. *J. Biol. Chem.* **275,** 31340–31346
26. Ishmukhametov, R. R., Galkin, M. A., and Vik, S. B. (2005) Ultrafast purification and reconstitution of His-tagged cysteine-less *Escherichia coli* F_1F_O ATP synthase. *Biochim. Biophys. Acta* **1706,** 110–116
27. Gumbiowski, K., Cherepanov, D., Muller, M., Panke, O., Promto, P., Winkler, S., Junge, W., and Engelbrecht, S. (2001) F-ATPase. Forced full rotation of the rotor despite covalent cross-link with the stator. *J. Biol. Chem.* **276,** 42287–42292
28. Mertens, N., Remaut, E., and Fiers, W. (1995) Tight transcriptional control mechanism ensures stable high-level expression from T7 promoter-based expression plasmids. *Biotechnology* **13,** 175–179
29. Nielsen, J., Hansen, F. G., Hoppe, J., Friedl, P., and von Meyenburg, K. (1981) The nucleotide sequence of the *atp* genes coding for the F_O subunits *a*, *b*, *c* and the F_1 subunit δ of the membrane-bound ATP synthase of *Escherichia coli*. *Mol. Gen. Genet.* **184,** 33–39
30. Brockmann, B., Koop genannt Hoppmann, K. D., Strahl, H., and Deckers-Hebestreit, G. (2013) Time-delayed *in vivo* assembly of subunit *a* into preformed *Escherichia coli* F_OF_1 ATP synthase. *J. Bacteriol.* 10.1128/JB.00468-13
31. Sambrook, J., and Russell, D. W. (2001) *Molecular Cloning: A Laboratory Manual*, 3rd Ed., p. A2.2, Cold Spring Harbor Laboratory, Cold Spring Harbor, NY
32. Dunn, S. D., Heppel, L. A., and Fullmer, C. S. (1980) The NH_2-terminal portion of the α subunit of *Escherichia coli* F_1 ATPase is required for binding the δ subunit. *J. Biol. Chem.* **255,** 6891–6896
33. Cagnon, C., Valverde, V., and Masson, J.-M. (1991) A new family of sugar-inducible expression vectors for *Escherichia coli*. *Protein Eng.* **4,** 843–847
34. Neidhardt, F. C., Ingraham, J. L., and Schaechter, M. (1990) *Physiology of the Bacterial Cell. A Molecular Approach*, pp. 1–29, Sinauer Associates, Sunderland, MA
35. Strahl, H., and Greie, J.-C. (2008) The extremely halophilic archaeon *Halobacterium salinarum* R1 responds to potassium limitation by expression of the K^+-transporting KdpFABC P-type ATPase and by a decrease in intracellular K^+. *Extremophiles* **12,** 741–752
36. Douglas, M., Finkelstein, D., and Butow, R. A. (1979) Analysis of products of mitochondrial protein synthesis in yeast. Genetic and biochemical aspects. *Methods Enzymol.* **56,** 58–66
37. Wise, J. G. (1990) Site-directed mutagenesis of the conserved β subunit tyrosine 331 of *Escherichia coli* ATP synthase yields catalytically active enzymes. *J. Biol. Chem.* **265,** 10403–10409
38. Pänke, O., Gumbiowski, K., Junge, W., and Engelbrecht, S. (2000) F-ATPase. Specific observation of the rotating *c* subunit oligomer of EF_OEF_1. *FEBS Lett.* **472,** 34–38
39. Schägger, H., and von Jagow, G. (1987) Tricine-sodium dodecyl sulfate-polyacrylamide gel electrophoresis for the separation of proteins in the range from 1 to 100 kDa. *Anal. Biochem.* **166,** 368–379
40. Birkenhäger, R., Greie, J.-C., Altendorf, K., and Deckers-Hebestreit, G. (1999) F_O complex of the *Escherichia coli* ATP synthase. Not all monomers of the subunit *c* oligomer are involved in F_1 interaction. *Eur. J. Biochem.* **264,** 385–396
41. Stalz, W.-D., Greie, J.-C., Deckers-Hebestreit, G., and Altendorf, K. (2003) Direct interaction of subunits *a* and *b* of the F_O complex of *Escherichia coli* ATP synthase by forming an ab_2 subcomplex. *J. Biol. Chem.* **278,** 27068–27071
42. Dmitriev, O., Jones, P. C., Jiang, W., and Fillingame, R. H. (1999) Structure of the membrane domain of subunit *b* of the *Escherichia coli* F_OF_1 ATP synthase. *J. Biol. Chem.* **274,** 15598–15604
43. Greie, J.-C., Deckers-Hebestreit, G., and Altendorf, K. (2000) Subunit organization of the stator part of the F_O complex from *Escherichia coli* ATP synthase. *J. Bioenerg. Biomembr.* **32,** 357–364
44. McLachlin, D. T., and Dunn, S. D. (1997) Dimerization interactions of the *b* subunit of the *Escherichia coli* F_1F_O-ATPase. *J. Biol. Chem.* **272,** 21233–21239
45. Eya, S., Maeda, M., and Futai, M. (1991) Role of the carboxyl terminal region of H^+-ATPase (F_OF_1) *a* subunit from *Escherichia coli*. *Arch. Biochem. Biophys.* **284,** 71–77
46. Pierson, H. E., Uhlemann, E.-M., and Dmitriev, O. Y. (2011) Interaction with monomeric subunit *c* drives insertion of ATP synthase subunit *a* into the membrane and primes *a-c* complex formation. *J. Biol. Chem.* **286,** 38583–38591
47. Jiang, W., Hermolin, J., and Fillingame, R. H. (2001) The preferred stoichiometry of *c* subunits in the rotary motor sector of *Escherichia coli* ATP synthse is 10. *Proc. Natl. Acad. Sci. U.S.A.* **98,** 4966–4971
48. Brandt, K., Maiwald, S., Herkenhoff-Hesselmann, B., Gnirss, K., Greie, J.-C., Dunn, S. D., and Deckers-Hebestreit, G. (July 11, 2013) Individual interactions of the *b* subunits within the stator of the *Escherichia coli* ATP synthase. *J. Biol. Chem.* 10.1074/jbc.M113.465633
49. Deckers-Hebestreit, G., Simoni, R. D., and Altendorf, K. (1992) Influence of subunit-specific antibodies on the activity of the F_O complex of the ATP synthase of *Escherichia coli*. I. Effects of subunit *b*-specific polyclonal antibodies. *J. Biol. Chem.* **267,** 12364–12369
50. Solomon, K. A., and Brusilow, W. S. (1988) Effect of an *uncE* ribosome-binding site mutation on the synthesis and assembly of the *Escherichia coli* proton-translocating ATPase. *J. Biol. Chem.* **263,** 5402–5407
51. Schneider, E., and Altendorf, K. (1984) Subunit *b* of the membrane moiety (F_O) of ATP synthase (F_1F_O) from *Escherichia coli* is indispensable for H^+ translocation and binding of the water-soluble F_1 moiety. *Proc. Natl. Acad. Sci. U.S.A.* **81,** 7279–7283
52. Schneider, E., and Altendorf, K. (1985) All three subunits are required for the reconstitution of an active proton channel (F_O) of *Escherichia coli* ATP synthase (F_1F_O). *EMBO J.* **4,** 515–518
53. Pati, S., and Brusilow, W. S. (1989) The roles of the α and γ subunits in proton conduction through the F_O sector of the proton-translocating ATPase of *Escherichia coli*. *J. Biol. Chem.* **264,** 2640–2644
54. Pati, S., Brusilow, W. S., Deckers-Hebestreit, G., and Altendorf, K. (1991) Assembly of the F_O proton channel of the *Escherichia coli* F_1F_O ATPase. Low proton conductance of reconstituted F_O sectors synthesized and assembled in the absence of F_1. *Biochemistry* **30,** 4710–4714
55. Fillingame, R. H., Porter, B., Hermolin, J., and White, L. K. (1986) Synthesis of the *Escherichia coli* H^+-ATPase does not require synthesis of the α and β subunits in F_1. *J. Bacteriol.* **165,** 244–251
56. Monticello, R. A., and Brusilow, W. S. (1994) Role of the δ subunit in enhancing proton conduction through the F_O of the *Escherichia coli* F_1F_O ATPase. *J. Bacteriol.* **176,** 1383–1389
57. Lau, W. C., and Rubinstein, J. L. (2012) Subnanometre-resolution structure of the intact *Thermus thermophilus* H^+-driven ATP synthase. *Nature* **481,** 214–218
58. Kucharczyk, R., Zick, M., Bietenhader, M., Rak, M., Couplan, E., Blondel, M., Caubet, S.-D., and di Rago, J.-P. (2009) Mitochondrial ATP synthase disorders. Molecular mechanisms and the quest for curative therapeutic approaches. *Biochim. Biophys. Acta* **1793,** 186–199
59. Price, C. E., and Driessen, A. J. (2010) Biogenesis of membrane bound respiratory complexes in *Escherichia coli*. *Biochim. Biophys. Acta* **1803,** 748–766
60. Dalbey, R. E., Wang, P., and Kuhn, A. (2011) Assembly of bacterial inner membrane proteins. *Annu. Rev. Biochem.* **80,** 161–187
61. Rak, M., Zeng, X., Brière, J. J., and Tzagoloff, A. (2009) Assembly of F_O in *Saccharomyces cerevisiae*. *Biochim. Biophys. Acta* **1793,** 108–116
62. Dunn, S. D., and Futai, M. (1980) Reconstitution of a functional coupling factor from the isolated subunits of *Escherichia coli* F_1 ATPase. *J. Biol. Chem.* **255,** 113–118
63. Sternweis, P. C. (1978) The ϵ subunit of *Escherichia coli* coupling factor 1

is required for its binding to the cytoplasmic membrane. *J. Biol. Chem.* **253,** 3123–3128
64. Schatz, G. (1968) Impaired binding of mitochondrial adenosine triphosphatase in the cytoplasmic "petite" mutant of *Saccharomyces cerevisiae*. *J. Biol. Chem.* **243,** 2192–2199
65. Tzagoloff, A. (1969) Assembly of the mitochondrial membrane system. II. Synthesis of the mitochondrial adenosine triphosphatase, F_1. *J. Biol. Chem.* **244,** 5027–5033
66. al-Shawi, M. K., Parsonage, D., and Senior, A. E. (1990) Adenosine triphosphatase and nucleotide binding activity of isolated β-subunit preparations from *Escherichia coli* F_1F_O-ATP synthase. *J. Biol. Chem.* **265,** 5595–5601
67. Feniouk, B. A., Suzuki, T., and Yoshida, M. (2006) The role of subunit epsilon in the catalysis and regulation of F_OF_1-ATP synthase. *Biochim. Biophys. Acta* **1757,** 326–338
68. Ono, S., Sone, N., Yoshida, M., and Suzuki, T. (2004) ATP synthase that lacks F_Oa-subunit. Isolation, properties, and indication of F_Ob_2-subunits as an anchor rail of a rotating *c*-ring. *J. Biol. Chem.* **279,** 33409–33412
69. Kuruma, Y., Suzuki, T., Ono, S., Yoshida, M., and Ueda, T. (2012) Functional analysis of membraneous F_O-*a* subunit of F_1F_O-ATP synthase by *in vitro* protein synthesis. *Biochem. J.* **442,** 631–638
70. Wittig, I., Meyer, B., Heide, H., Steger, M., Bleier, L., Wumaier, Z., Karas, M., and Schägger, H. (2010) Assembly and oligomerization of human ATP synthase lacking mitochondrial subunits a and A6L. *Biochim. Biophys. Acta* **1797,** 1004–1011
71. Brusilow, W. S. (1993) Assembly of the *Escherichia coli* F_1F_O ATPase, a large multimeric membrane-bound enzyme. *Mol. Microbiol.* **9,** 419–424
72. Dunn, S. D., and Chandler, J. (1998) Characterization of a $b_2\delta$ complex from *Escherichia coli* ATP synthase. *J. Biol. Chem.* **273,** 8646–8651
73. Wilkens, S., Dunn, S. D., Chandler, J., Dahlquist, F. W., and Capaldi, R. A. (1997) Solution structure of the N-terminal domain of the δ subunit of the *E. coli* ATP synthase. *Nat. Struct. Biol.* **4,** 198–201
74. McLachlin, D. T., Bestard, J. A., and Dunn, S. D. (1998) The *b* and δ subunits of the *Escherichia coli* ATP synthase interact via residues in their C-terminal regions. *J. Biol. Chem.* **273,** 15162–15168